hydrodynamic loss driven by giant impact. In preparation.
Pollack, J. B., et al. 1993. Near-infrared light from Venus' nightside: A spectroscopic analysis. *Icarus* 103:1–42.
Prinn, R. G., and Fegley, B., Jr. 1989. Solar nebula chemistry: Origin of planetary, satellite and cometary volatiles. In *Origin and Evolution of Planetary and Satellite Atmospheres*, eds. S. K. Atreya, J. B. Pollack and M. S. Matthews (Tucson: Univ. of Arizona Press), pp. 78–136.
Revercomb, H. E., Sromovsky, L. A., Suomi, V. E., and Boese, R. W. 1985. Net thermal radiation in the atmosphere of Venus. *Icarus* 61:521–538.
Rodriguez, J. M., Prather, M. J., and McElroy, M. B. 1984. Hydrogen on Venus: Exospheric distribution and escape. *Planet. Space Sci.* 32:1235–1355.
Shoemaker, E., and Wolfe, R. 1982. Cratering time scales for the Galilean satellites of Jupiter. In *The Satellites of Jupiter*, ed. D. Morrison (Tucson: Univ. of Arizona Press), pp. 277–339.
Shoemaker, E., Wolfe, R., and Shoemaker, C. 1990. Asteroid and comet flux in neighborhood of Earth. In *Global Catastrophes in Earth History*, eds. V. L. Sharpton and P. D. Ward, GSA SP-247 (Boulder: Geological Soc. of America), pp. 155–170.
Shoemaker, E., Weissman, P., and Shoemaker, C. 1994. The flux of periodic comets near Earth. In *Hazards Due to Comets and Asteroids*, ed. T. Gehrels (Tucson: Univ. of Ariona Press), pp. 313–335.
Watson, A. J., Donahue, T. M., and Walker, J. C. G. 1981. The dynamics of a rapidly escaping atmosphere: Applications to the evolution of Earth and Venus. *Icarus* 48:150–166.
Wetherill, G. W. 1991. Formation of the terrestrial planets from planetesimals. In *Planetary Sciences: American and Soviet Research*, ed. T. M. Donahue (Washington, D. C.: National Academy Press), pp. 98–115.

From: Venus II. 1997. Ed. S. W. Bougher, D. M. Hunten, and R. J. Phillips. Tucson, Univ. of Arizona Press.

CHEMISTRY OF LOWER ATMOSPHERE AND CLOUDS

LARRY W. ESPOSITO
University of Colorado

JEAN-LOUP BERTAUX
Service d'Aeronomie CNES

VLADIMIR KRASNOPOLSKY
Goddard Space Flight Center

and

V. I. MOROZ and L. V. ZASOVA
Space Research Institute, Russian Academy of Sciences

Venus is totally covered by clouds, up to 60 km in vertical extent. The photochemistry that creates the cloud aerosols grades into thermal chemistry that is dominant below the upper clouds. We review selected measurements from Venera, Vega, Hubble Space Telescope (HST) and groundbased telescopes that constrain the chemistry of the lower atmosphere and clouds. The *in-situ* Vega measurements of SO_2 abundance in the deep atmosphere are at variance with earlier gas chromatograph measurements and with present chemical models. Russian and American measurements of SO_2 in the upper cloud have been reconciled. SO_2 continues its long decline seen since 1978 above the cloud tops. We review chemical models of the atmosphere above the clouds and recent progress in modeling of the cloud layer and sub-cloud atmosphere. We still do not know the species responsible for Venus' blue absorption. The existence of large and/or crystalline size modes of cloud particles is still open. Advances in understanding Venus atmospheric chemistry will require future measurements of sulfur and chlorine compounds.

The effort to determine the composition and chemistry of the Venus atmosphere had been an objective of numerous space missions to Venus and extensive ground-based telescopic observations. In this chapter, we review some of the recent data bearing on the chemistry of the lower atmosphere and cloud region (with particular emphasis on data from Venera 15, Vega 1 and 2, and ultraviolet spectroscopy). We discuss the chemical models that have been developed to explain the observations in this region, and draw some critical comparisons among them.

Some of the most important new information of the last decade has come from near-infrared measurements of the Venus night side, which probe the deeper Venus atmosphere through windows in the CO_2 absorption spectrum.

The nightside emissions at 1.7 and 2.3 μm discovered by Allen and Crawford (1984) were readily identified (see, e.g., Krasnopolsky 1986, p. 181) as spectral windows to the lower atmosphere. Later, windows at 1.31, 1.27, 1.18, and 1.01 μm were found, and lines of CO_2, H_2O, HDO, SO_2, CO, OCS, HCl, and HF have been identified. These data are discussed in more detail in the chapters by Taylor et al. and by Crisp and Titov. In this chapter, we restrict our attention to the Venus atmosphere below 90 km; the chemistry above this altitude is discussed in the chapters by Fox et al. and by Bougher et al. The mesosphere is discussed in the chapter by Lellouch et al.

The Venus clouds and hazes have enormous vertical extent, with a lower haze down to ~30 km and an upper thick haze up to 90 km altitude; the entire system covers a vertical depth of ~60 km, with the average visibility in the Venus clouds better than several km. The main cloud deck extends from ~70 km (the level of unit optical depth in the ultraviolet) down to altitudes between 45 to 50 km.

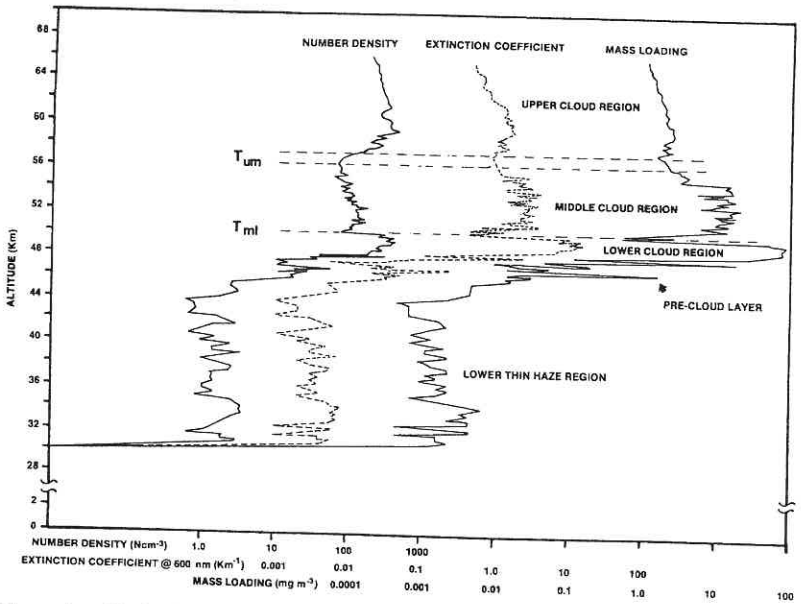

Figure 1. Vertical structure of the Venus atmosphere from direct computations based on the Pioneer Venus LCPS data (Knollenberg and Hunten 1980). The boundaries between the upper and middle cloud, T_{um} (about 1 km) and the middle and lower T_{ml} (several hundred meters) are shown. The mass loading is calculated for a density of 2 g cm^{-3}.

Spacecraft *in-situ* measurements allow us to divide the cloud system into upper, middle and lower clouds (see Fig. 1 and Esposito et al. 1983). Considering all the Pioneer Venus (PV) and Venera nephelometer results and the LCPS (Pioneer Venus Cloud Particle Size Spectrometer) measurements,

it appears that the middle and upper cloud structure are planetwide features. In all cases the opacity is higher in the middle than upper cloud, typically by a factor of 2. The lower cloud is well defined and highly variable from location to location. Sharp layers are evident and these have the highest opacity at the Pioneer Large and Night probe sites.

The clouds within the main deck would all be thin stratiform in terrestrial classification. Instabilities are slight and latent convection potential is negligible (see Knollenberg et al. 1980). Only the middle cloud region appears to have any potential for convective overturning.

The chemistry of the lower Venus atmosphere divides naturally into three regions. In the main cloud layers above 60 km, photon-driven processes are important, and the term "photochemistry" applies well here. Below the clouds, thermal processes and vertical transport are key, and this region is dominated by "thermal chemistry." At the lower altitudes, interactions with the surface may dominate.

The recent reviews of Venus atmospheric chemistry by Prinn (1985) and Krasnopolsky (1986) are not outdated; the reader is referred to these for more detail on a number of chemical processes discussed in this chapter. The material in this chapter is divided into the following three sections: selected recent observations; the atmospheric chemistry; and open questions.

I. SELECTED RECENT OBSERVATIONS

A. Results from Venera 15 and Vega 1 and 2

1. Introduction. Venera 15 and 16 were launched in 1983. Both spacecraft were inserted on elliptical orbits around Venus. The main goal of this twin mission was mapping the Venus surface in the northern hemisphere with synthetic aperture radar (SAR). However, two atmospheric experiments were also included: observations of the thermal radiation spectra and radio-occultation measurements. Spectrometric observations were successful only on Venera 15. The instrument failed after two months on orbit, but considerable information about the temperatures, aerosols, sulfur dioxide and water vapor in the upper clouds and above was obtained in this short period of time.

Two years later (1985) the Vega 1 and Vega 2 spacecraft flew by Venus on their way to Halley's comet. As they passed Venus, each of them delivered two descent and two balloon probes. A set of *in-situ* atmospheric studies that included balloon experiments gave the first horizontal profiles of the Venusian atmosphere in the cloud region.

A short description of the Vega balloons and their preliminary results were presented by Sagdeev et al. (1986), and for Vega descent probes by Deriugin et al. (1987) and Moroz (1987). These spacecraft provided the last point in the long history of the studies of Venus by Soviet missions: 13 successful entry vehicles (including 10 with soft landings) beginning in 1967, when Venera 4 provided the first *in-situ* studies of another planet.

The following short review of the results of atmospheric studies on Venera 15 and Vega 1, 2 missions emphasizes the new findings useful to update the descriptions of the chemical composition of gas, clouds and hazes published more than 10 years ago in the *Venus* book (Hunten et al. 1983) by von Zahn et al. (1983) and Esposito et al. (1983).

2. *Infrared Spectra Measured by Venera 15: Observational Results and Interpretation.* The infrared Fourier spectrometer (FS) on board the Venera 15 orbiter (Moroz et al. 1986; Oertel et al. 1987) covered a spectral range from 270 to 1600 cm^{-1} (6–35 μm). The field of view of the instrument corresponded to an area about 100×100 km in the polar region. The goal of this experiment was to study the planet's thermal radiation spectra with higher spectral resolution (5–7 cm^{-1}) and continuous spectral coverage compared to the previously available thermal infrared spectra of Venus from the Earth (see, e.g., Kunde et al. 1977). Terrestrial measurements were not disk resolved and were corrupted by strong terrestrial absorptions; those of Venus were from filter spectroscopy of the PV OIR experiment (Taylor et al. 1980).

Venera 15 observed mainly the northern hemisphere, but a few tens of spectra were obtained in the equatorial region and south mid-latitudes. The total number of available spectra exceeds 1500. Some representative examples are shown in Fig. 2. Absorption bands of three atmospheric gases (CO_2, H_2O and SO_2) and also H_2SO_4 aerosols are clearly visible. The very strong 15 μm CO_2 band has different morphology at different locations, mostly owing to variability of the temperature profiles. Band center emission arises from atmospheric layers at about 90 km altitude. Differences are clearly visible in the continuum between the bands. These reflect variability in vertical structure of the upper clouds and haze.

Interpretation of FS data appears in a set of works from the last decade (Moroz et al. 1985,1986,1990; Spankuch et al. 1985,1990; Zasova et al. 1985,1989,1993; Schaefer et al. 1987,1990; Linkin et al. 1985). Their general approach included the following:

(1) Upper cloud and upper haze particles are presumed to consist of sulfuric acid water solutions. This critical assumption was confirmed by the good agreement of synthetic and observed spectra.

(2) The spectral dependence of the extinction coefficient is computed from the assumption that the particle size distribution corresponds to the measured "mode 2" from the PV LCPS, with parameters as proposed by Pollack et al. (1980) (log-normal distribution with mean cross-section weighted size r = 1.05 μ and variance σ = 1.21).

(3) CO_2 pure gas transmission functions for a set of channels within the 15 μm band are combined with computed aerosol transmission functions. Then an iteration procedure (e.g., using relaxation as by Zasova et al. [1989]) is adopted for the simultaneous retrieval of the temperature and aerosols profiles.

(4) Temperature and aerosol profiles retrieved by step (3) can be used to compute synthetic spectra for the SO_2 and H_2O bands, which allow us to derive their abundances (see below Sec. I.A.4).

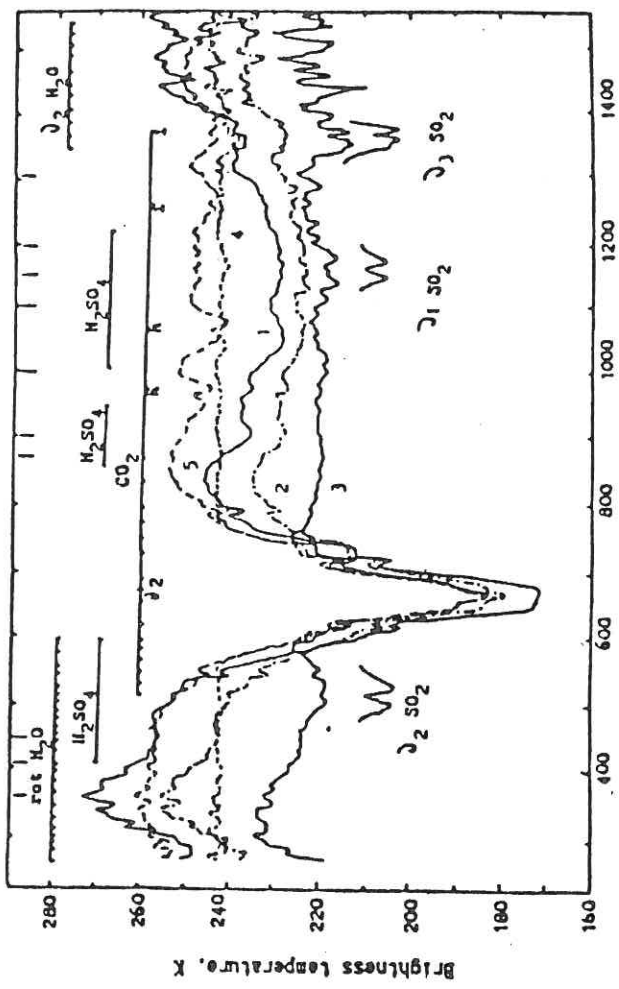

Figure 2. Venera 15 FS (infrared spectrometer experiment) brightness temperature vs wavenumber for five characteristic groups of spectra, averaged within latitude zones: 1 is for equatorial zone; 2 for 30 to 50°, 3 for "cold collar" on 60 to 80°, 4 is typical for near polar region; 5 for hot high-latitude regions (dipole?). From 5 to 12 spectra were averaged in each latitude bin. Some of the spectra observed between 50 and 80°N but outside of the cold collar can be explained as a linear combination of type (2) and (4) (Zasova et al. 1993). This means that the horizontal structure of clouds consists of small unresolvable spots having different vertical cloud structure.

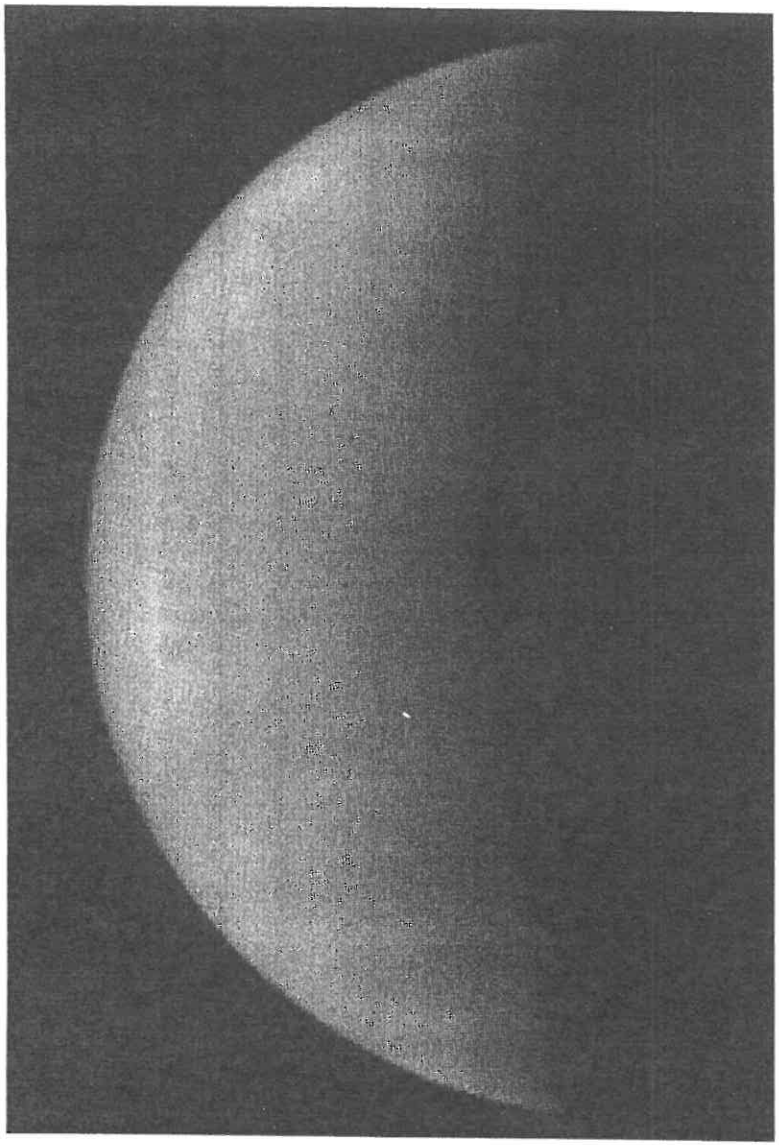

Figure 3. Hubble image of Venus (WFPC2 at 255 nm) from 25 January 1995. Note the muted contrasts and similarity to previous ultraviolet images (see, e.g., Rossow et al. 1980) (figure from Na and Esposito 1996).

3. Vega Experiments Concerning Clouds, Hazes and Atmospheric Chemistry. Much new information about winds and turbulence was obtained from ground radiotracking of the balloons and *in-situ* measurements. Those parts of the balloon results are outside of the scope of this chapter. However, the balloons provided the first *in-situ* nephelometric measurements for long horizontal paths (Sagdeev et al. 1986) and this was an important achievement in Venusian clouds studies.

Most of the atmospheric experiments on the descent probes targeted aerosols studies, including: (a) combined particle size spectrometer/nephelometer ISAV-A (Gnedyk et al. 1987*a,b*); (b) particle size spectrometers LSA, prepared by another team (Zhulanov et al. 1987); (c) gas-chromatograph (SIGMA-3) with aerosol collector (Porshnev et al. 1987); (d) mass-spectrometer (MALAHIT) with aerosol collector (Surkov et al. 1987); and (e) X-ray fluorescent analyzer IFP, also with an aerosol collector (Andreichikov et al. 1987).

All three instruments for chemical analysis of particle composition employed aerosol filters on their intakes to trap small particles during the descent of the probe through the atmosphere. Heating converted the collected material into the gas phase which were input to SIGMA-3 and MALAHIT. Both of these instruments were targeted mainly toward the *in-situ* detection of sulfuric acid, and this was actually accomplished (see below). IFP provided an analysis of the elemental composition of cloud particles. SIGMA-3 and IFP worked successfully on both probes, MALAHIT only on Vega 1.

All instruments mentioned above ceased their measurements between the altitudes of 35 and 45 km because they were mounted in a special section of the probe with only limited pressure and temperature protection.

The ultraviolet spectrometer ISAV-1 and 2 were used for sulfur dioxide measurements (Bertaux et al. 1987; Widemann et al. 1993; Bertaux et al. 1996) and humidity sensors for water vapor measurements (Surkov et al. 1987). Two different type sensors ("thermoelectrical" and "electrometrical") were used for water vapor measurements on both probes.

The landing sites of the Vega 1, 2 descent probes were located on the night side of the planet, in contrast to all previous Soviet missions to Venus beginning with Venera 9 and 10.

4. Sulfur Dioxide and Water Vapor Measurements. SO_2 was first detected in the atmosphere of Venus by Barker (1979) with groundbased observations, and it was subsequently confirmed by Stewart et al. (1979) and Conway et al. (1979). The abundances of SO_2 in 1978–1979 were larger than the previously established upper limits (Owen and Sagan 1972) by orders of magnitude. Continuous observations by Pioneer Venus from 1978 to 1986 showed a steady decline in the cloud top SO_2 abundance toward values consistent with previous upper limits (Esposito et al. 1988). This decline has been confirmed by IUE observations (Na et al. 1990) and by HST (Na and Esposito 1996); see Figs. 3, 4 and 5. The preliminary analysis of SO_2 abundance from HST is less than 25 ppb at the cloud tops (Na and Esposito 1996). Figure 5 is a compilation

of SO_2 cloud-top measurements. Explanations that have been advanced for the likely rapid increase and observed slow decline of SO_2 include active volcanism (Esposito 1984) and changes in atmospheric dynamics (Clancy and Muhleman 1991). The volcano hypothesis uses the volcanic eruption as a source of bouyancy that allows the abundant SO_2 below the Venus clouds to break through the stable upper cloud layer. This entrained SO_2 is then visible remotely to ultraviolet observations at the cloud top. The SO_2 abundance below the clouds varies much more slowly, related to the amount of volcanic activity over geologic time scales of millions of years (see the chapter by Fegley et al.). It is therefore puzzling why a similar reduction is seen between the Pioneer Venus and Venera 12 *in-situ* measurements of 1978 and the Vega results in 1986.

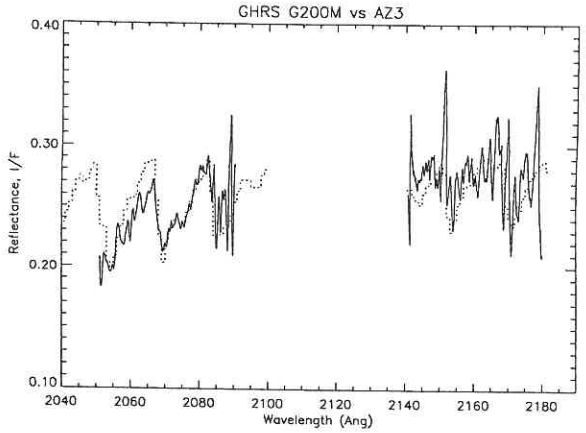

Figure 4. Hubble spectrum of Venus (GHRS G200M at 207 nm and 216 nm) from 1995 observations. Overplotted is a model spectrum for 12.5 ppb SO_2 at 40 mb with an SO_2 scale height of 3 km (figure from Na and Esposito 1996).

The changes in SO_2 above and within the clouds of Venus may have a significant effect on the photochemistry of the clouds of Venus. Pioneer Venus observations have shown that the clouds of Venus are created by the photochemical processes that oxidize upwelling SO_2 (Winick and Stewart 1980; Yung and DeMore 1982; see Sec. II). Thus, any significant changes in SO_2 may have an effect on the chemistry and dynamics of the clouds.

Venera 15 FS vs Pioneer Ultraviolet Spectroscopy. Three new sulfur dioxide absorption bands were found in the spectra observed by FS: about 519, 1150 and 1360 cm^{-1} (the strongest). All the ultraviolet observations have shown that, for the cloud-top level of 40 mb (height about 69 km), sulfur dioxide is more abundant at low latitudes, and is much less observable at latitudes more than 50° (see, e.g., Esposito et al. 1979).

Venera 15 FS observations gave the opposite result; the infrared sulfur

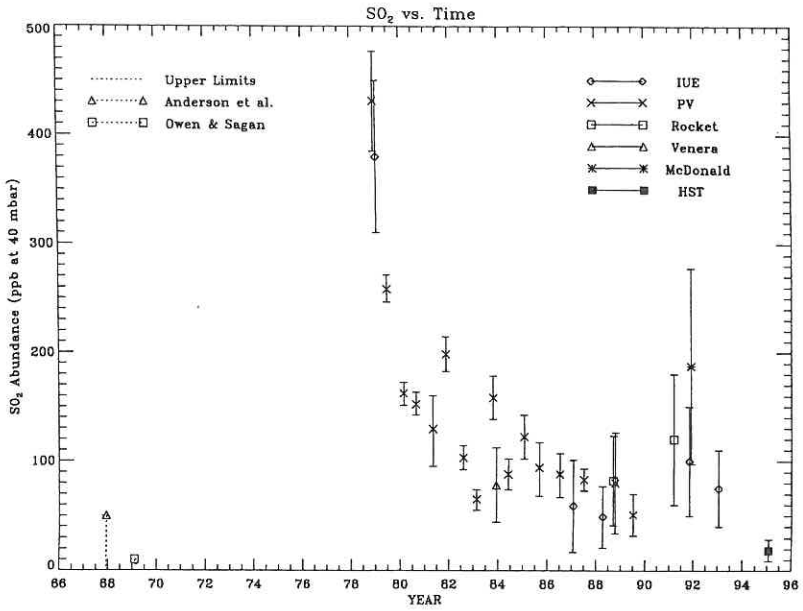

Figure 5. SO_2 abundance at 40 mb from 1968 to 1995, including groundbased, spacecraft and rocket measurements. Only upper limits were given by measurements prior to 1978 (left hand side of figure) (figure from Na and Esposito 1996).

dioxide bands were much more pronounced at high latitudes than at low. The shape and equivalent width of a band in thermal emission depends not only on the abundance of the corresponding gas but also on the temperature and aerosol extinction profiles. Fortunately, all of these can be obtained from the same spectrum in which the SO_2 bands are seen (see Fig. 6). The first attempts to retrieve the SO_2 abundances from these spectra did not show any pronounced latitude dependence for the heights 60 to 62 km (Moroz et al. 1990).

A joint analysis of both sets of data to resolve the apparent disagreement between the Venera 15 and PV OUVS SO_2 distribution was carried out by a small IKI/University of Colorado working group, and included the most recent observations from U. S. sounding rockets (McClintock et al. 1994; Na et al. 1994). The final conclusion (Zasova et al. 1993) is that all of the observations are consistent with the following latitude distribution. Around 1983, at the 40 mb (69 km) level, the SO_2 mixing ratio is a few tens of ppb at the low and middle latitudes (below 45°, approximately), 1 to 10 ppb in the cold collar and 100 to 200 ppb in the near polar hot regions ("dipole"), and in some places it reaches about 1000 ppb (Fig. 7).

The same analysis for the level 150 mb (62 km) yields the mixing ratio of 0.3 to 0.5 ppm at low and middle latitudes and increases to 1 to 2 ppm in

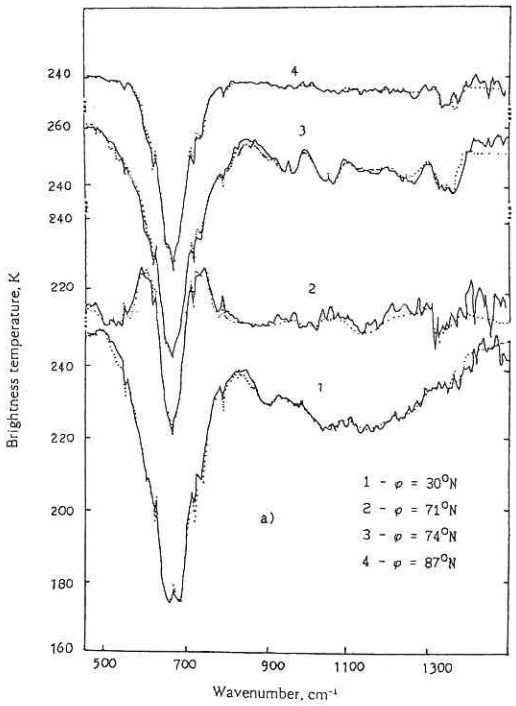

Figure 6. (a) Four individual Venera 15 FS spectra and (b) temperature and aerosol profiles derived from them. Dotted lines in part (a) are the derived synthetic spectra.

the polar region. The scale height of SO_2 is 1.5 to 2.5 km at low latitudes. The mixing ratio and scale height derived for middle latitudes are in good agreement with photochemically predicted values (Yung and DeMore 1982).

These two altitude reference levels (near 62 and 69 km) were selected because the first one is close to the lower boundary where the infrared measurements are sensitive to the vertical SO_2 profile and the second one is close to the upper boundary. The upper reference level is also convenient for comparison with ultraviolet observations (Fig. 8). At latitudes above 50 degrees the scale height varies from 1 to 6 km showing some pronounced correlation with the SO_2 mixing ratio.

The slant geometry typical for the high-latitude PV OUVS observations can explain the smaller amount of ultraviolet SO_2 absorption seen there. So, at the moment we have removed the controversy in understanding of the sulfur dioxide horizontal distribution at the level of the cloud tops. However, some of the discrepancies between ultraviolet and infrared remain. The SO_2 scale height from infrared data at high latitudes is 3 to 5 km, from ultraviolet it is about 1 km. At low latitudes, a rather good ultraviolet-infrared agreement was established for both the abundances, and for SO_2 scale height: here it is about 1.5 to 2.5 km. Different observational geometry and vertical variation of scale height (it could decrease above 69 km) can probably explain the remaining disagreement. Temporal variations are also very possible, because the Venera

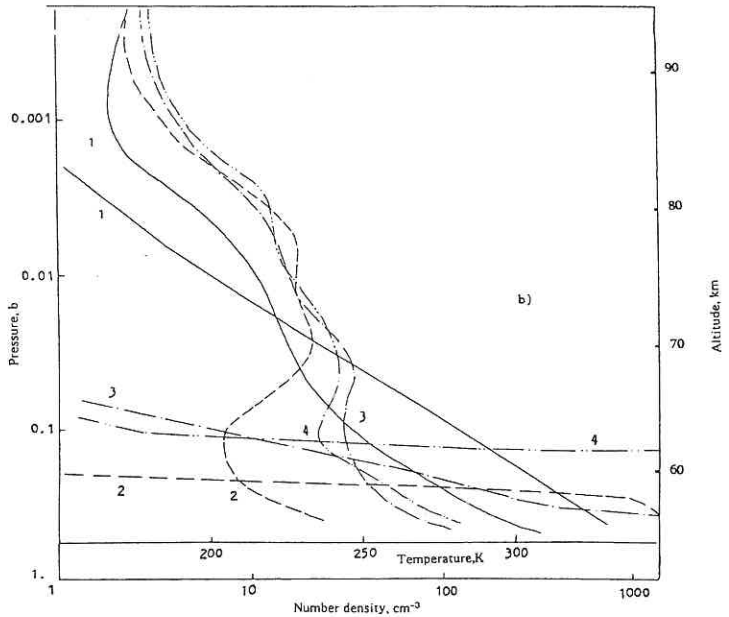

15 FS data are from a single two-month period in 1983.

Water Vapor Estimations from Venera 15 Infrared Spectra. Water vapor features are visible on all Venera 15 FS spectral records at wavenumbers below 400 cm^{-1} (wavelengths greater than 25 μm). These features show the short wavelength edge of the H_2O pure rotational band. The depth of these features varies, but a systematic effort to separate mixing ratio of H_2O from cloud variations (as was done for SO_2 bands) has still not been carried out. Tentative analysis (Moroz et al. 1990) showed that H_2O abundance at altitudes 58 to 60 km is 20±10 ppm and the scale height is between 2 and 3 km at altitude 58 km. Local mixing ratio variations up to a factor of 5 are possible. There is no clear conclusion about latitude variations. There is definitely no diurnal variation of the water vapor abundance.

The estimated mixing ratio 20±10 ppm at heights 58 to 60 km is in approximate agreement with the results of the analysis of PV OIR data (Schofield et al. 1982). However, there is no confirmation of any substantial increases of H_2O abundance (to 40 ppm) at night, as derived from OIR data. Moreover, it is not clear how water vapor and cloud absorptions could have been unambiguously separated using only the broadband filters of the OIR instrument.

The fundamental rotation-vibration water absorption band near 6.3 μm is also visible on Venera 15 FS spectra but the signal-to-noise ratio is here much poorer than for the pure rotational band.

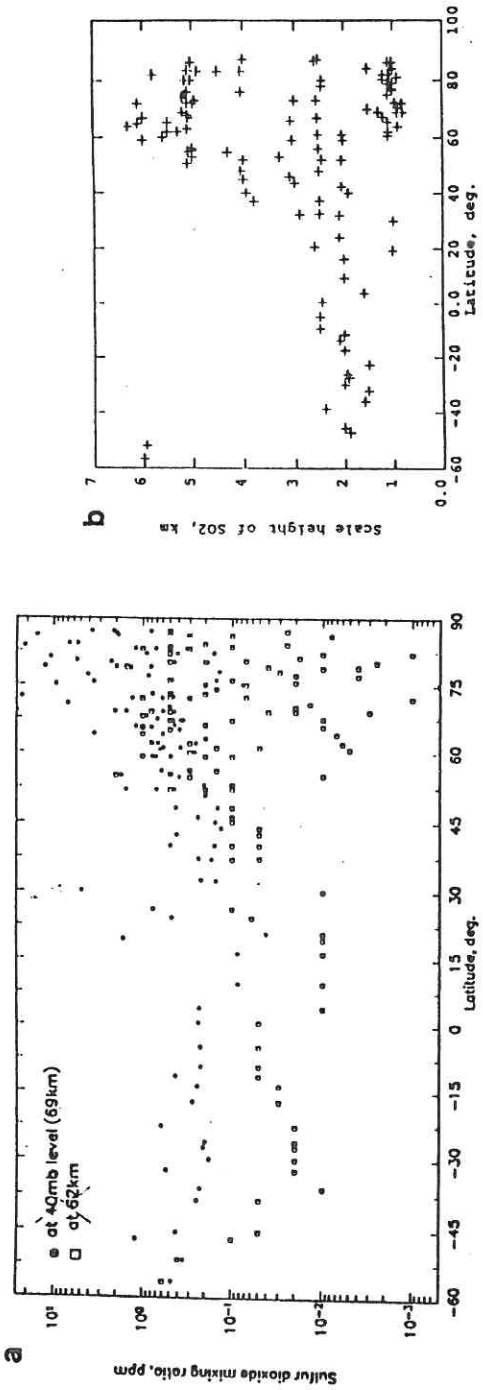

Figure 7. (a) The sulfur dioxide mixing ratio at 69 km (40 mb) vs latitude is given by filled circles, and the same at 62 km (150 mb) by squares. (b) scale height of the sulfur dioxide vs latitude (figure from Zasova et al. 1993).

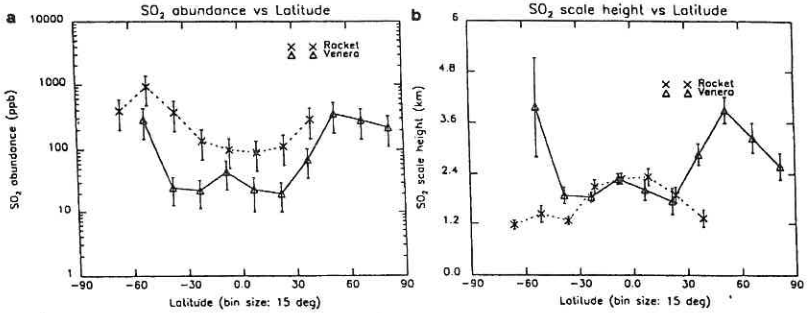

Figure 8. Comparison of the infrared Venera 15 FS and ultraviolet rocket data averaged over 15 degree latitude bins: (a) mixing ratio, (b) scale height (figure from Zasova et al. 1993).

Water Vapor from Vega Humidity Sensors. New *in-situ* H_2O measurements were also made by Vega 1 and 2 sounding/landing probes (Surkov et al. 1987). Surprisingly large abundances (about 1000 ppm with $\pm 50\%$ error bar) were found between 52 and 60 km. One of the proposed explanations was the absence of photochemical reactions at night. However, Venera 15 FS data do not show any daily variations, as was mentioned in the previous section. Maybe these very large abundances are really artifacts created by other constituents (cloud particles), but this was never checked by any additional analysis.

At heights 30 to 45 km the same humidity sensors have measured abundances of about 150 to 200 pm on both probes. These values are compatible with those obtained in previous missions (see reviews in Hunten [1983]) but are too high in comparison with those inferred from the near-infrared night glow spectra (see below).

5. Clouds and Hazes: Aerosol Profiles Inferred from Infrared Venera 15 FS Spectra. Brightness temperature (Tb) spectra of the thermal emission of Venus obtained in Venera 15 infrared experiment at low and high latitudes show significant differences in the characteristics of the continuum, visibility of hot CO_2 bands, and so forth (Fig. 2). This diversity can be partly explained by differences in the corresponding vertical temperature profiles. Aerosol vertical profiles would need to be different there also. The main properties of upper clouds and haze derived from infrared measurements (Zasova et al. 1993) are given in Table I.

Vega Descent Probes Nephelometer and Particle Spectrometer Results. The particle size distribution was measured by one of two particle size spectrometers of the Vega probes (ISAV-A; Gnedykh et al. 1987) at heights 48.5 to 52 km ("lower cloud"). This distribution can be matched by a superposition of two different size spectra: mode 1, with the relation between diameter D

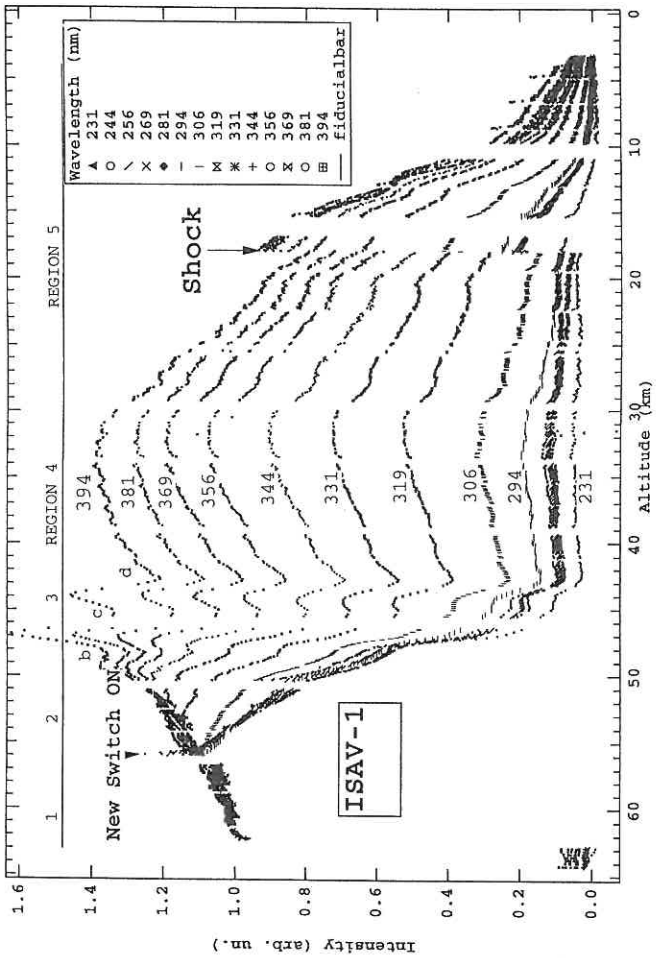

Figure 9. Vega ISAV-1 data as a function of altitude in the Venus atmosphere. Lightcurves for different wavelengths have been normalized to unity at altitude $z = 62.5$ km. In the region $20<z<40$ km, the lightcurves are in decreasing order of wavelength, with $\lambda = 394$ nm at the top. The event at $z = 18$ km where all lightcurves simultaneously increase is interpreted as a mechanical shock that released Venus aerosols collected on the ISAV optics at cloud altitudes. At both $z = 56$ km and $z = 50$ km, several wavelengths show a sharp increase, which disappears in about 20 s. This is interpreted as a spurious instrument effect occurring just after a new switch-on of the xenon flash. Five different regions (see Table II) are identified from the lightcurve variation. Narrow absorbing layers in the $\lambda = 394$ nm curve are labeled b, c, d (figure from Bertaux et al. 1996).

TABLE I

Aerosol Scale Height and Unit Optical Depth from Venera 15 FS

Latitude	Aerosol Scale Height (km)	Altitude of Unit Optical Depth for Two Wavenumbers (km)	
		365 cm^{-1}	1152 cm^{-1}
Less than 55°	3.5–4	57–59	67–69
55 to 75°			
Cold collar	<1	58–60	60–62
Inhomogeneous regions	<4	56–60	70–72
75 to 85°			
Hot dipole	1–1.5	56–58	59–64
Outside of dipole	<1	61–63	63–64
Greater than 80°	0.5	62–64	62–64

and number density N given by

$$dN(D)/dD = \text{const}^* \; D^n \tag{1}$$

with $n = 5\pm1$ for Vega 1 and 4 ± 1 for Vega 2. Mode 2 is as described by Pollack et al. 1980, although this gives some excess of particles with sizes between 1.5 and 4 μm.

This distribution differs from results of a similar experiment on the Pioneer Large probe (LCPS, Knollenberg and Hunten 1980). The LCPS identified a "mode 3," with sizes more than 5 μm as most important for the cross section and mass loading in lower clouds. There is a continuing controversy about the reality of mode 3 as a separate peak in the size distribution (the other possibility is that they can be described as a tail of some smooth size spectrum; see below, Sec. III.B), but there is no doubt of the presence of some large particles and their role in the integrated properties of Venusian clouds. Large particles also were not identified in the data of the second particle spectrometer (LSA; Zhulanov et al. 1986). There is a suspicion that most of large particles were simply missed in both of these experiments because they did not have a special channel to measure them as did the LCPS. The integrated number densities ($D>0.8$ μm) are nearly the same as measured by LCPS at heights above 48.4 km, but are 30 times larger below 48 km. These experiments detect no sharp boundary at the lower cloud bottom, as has been identified in many previous missions beginning from Venera 9 and 10. Nephelometric data also do not show this boundary.

So the absence of the sharp lower boundary of the main cloud deck is probably a real feature of the aerosol vertical structure above the Vega 1 and 2 landing sites. Previous data provide only one instance where the lower cloud boundary was not found, in the Venera 8 mission. Perhaps this peculiarity is

connected with the local time; both Vega landings were done in late night and Venera 8 was near the terminator. However, the Night Probe nephelometer on Pioneer Venus did not show any difference in cloud structure compared with those obtained during daytime.

ISAV-A provided simultaneous measurement of the light scattered by individual particles in four directions: forward, back and two with 90° scattering angle and 90° azimuthal difference. Comparison of signals in the two last channels provided a possibility to discriminate between spherical (liquid) and nonspherical particles. It was found that majority of particles with $D>0.8\,\mu$m are spherical.

Comparison of signals corresponding to three different scattering angles provided estimations of the refractive index m. All particles with $D>2\,\mu$m had $m = 1.4\pm05$. Particles with diameters $0.8<D<2\,\mu$m can be separated in two groups: (1) with $m = 1.4\pm0.1$ (about 80% of registered events), and (2) with $m = 1.7\pm0.1$ (about 20%). No height dependence was found for these properties, but most of the particles were measured in the lower and middle clouds.

Vega Balloon Nephelometer Results. Simple nephelometers were included in the Vega balloon instrumental package. A backscattering coefficient about 1.5×10^{-4} m^{-1} sr^{-1} was measured at the height the balloons floated (54.5 km), in approximate agreement with nephelometers on the Vega landers. These measurements showed that middle clouds are horizontally very homogeneous near the equatorial region of the planet.

Chemical Composition of Particles: Sulfuric Acid. Venera 15 FS spectra provided a strong confirmation of an aqueous solution (75–85%) of sulfuric acid as the particulate material in the upper clouds. Otherwise, such good coincidence of synthetic and observed spectra would be impossible (see Fig. 6a).

The first in situ detection of sulfuric acid was made in experiments SIGMA-3 and MALAHIT. The analysis of SIGMA-3 results yields the average mass density of sulfuric acid about 1 mg m^{-3}, estimated for heights 48 to 54 km and "much lower" at about 54 km (Porshnev et al. 1987). Conclusions from MALAHIT analysis are even less definite and not in a good agreement with SIGMA-3 results; they give an average mass density between 2 and 10 mg m^{-3} (Surkov et al. 1987). Neither experiment can say anything about the upper clouds.

Chemical Composition of Particles: Other Constituents. Very interesting results (but quite difficult for quantitative interpretation) were obtained by elemental X-ray analysis of the thin layers collected by the IPF experiment (Andreichikov et al. 1987). Three elements were identified: sulfur, chlorine and phosphorus. Sulfur and chlorine in cloud particles had been detected previously by similar measurements, but not phosphorus. It is clear that some P-bearing substance can be important as a particulate in lower clouds. Phosphoric acid H_3PO_4 is a likely candidate for this substance and phosphorous anhydride P_4O_6 may be the gas responsible for its production (Andreichikov

1987). A critical review of these data was given by Krasnopolsky (1989). The key conclusion in the paper is that the lower subcloud boundary at the level about 33 km registered on Venera 8 and later on some other missions can be explained by phosphoric acid particles dominating in the subclouds.

The refractive index 1.7 estimated for some of the particles registered in ISAV-A experiment can be understood if they consist of free condensed sulfur. Some evidence for the presence of free sulfur in clouds were obtained from the analysis of the SIGMA-3 and IPF results.

B. ISAV Measurements of Ultraviolet Absorption

1. Introduction. The ISAV spectrometer (220–400 nm) was a part of the optical instrumentation flown on board the two Vega descent probes, together with the ISAV-A equipment dedicated to the aerosol cloud particles, for which results have been reported elsewhere (Moshkin et al. 1986; Gnedykh et al. 1987; see above).

The fly-by geometry at Venus was constrained by the later encounter with comet Halley, and as a result, the atmospheric probes were released on the night side of Venus. This was an ideal situation to conduct an "active spectroscopy" experiment, in which the ultraviolet spectrum of an artificial light source was continuously measured after traversing a gas-cell of 1.70 m path length, within which was circulated the ambient atmosphere all along the descent.

Useful measurements were made from 62.5 km of altitude down to the ground, with a vertical resolution ranging from 40 to 180 m, thanks to the relatively high sampling rate (one spectrum every 4 s). This was the first time such an instrument was flown in another planet's atmosphere, and we do not expect to have new opportunities to repeat it in the foreseeable future.

The results presented by Bertaux et al. (1996) rely on a number of assumptions made about the behavior of the instrument and the descent probe during its course to the ground. Bertaux et al. present both their primary data and their interpretation of the data along with a detailed discussion of the assumptions involved, in such a way that the reader may be able to establish his own opinion about the data and their conclusions. Because of the uniqueness of the observations, this interpretation deserves serious attention.

2. Discussion of the Light Curves. A total of 584 "short" spectra were acquired for ISAV-1 and 594 for ISAV-2 during the flights, at a constant rate of one every 4 seconds (except for a small interruption every 200 s for 20 s). All normalized lightcurves $I(\lambda_j, z)$ are shown on Fig. 9 for ISAV-1 and for λ_j varying from 231 to 394 nm, as a function of altitude above the landing point. The spread of the individual points along a lightcurve is representative of the total instrumental noise and is in most cases quite small.

Bertaux et al. (1996) identify several features in the lightcurves as purely instrumental. The rest of the intensity variations are interpreted as arising from gaseous absorption, along with the effect of a deposit of cloud particles on the instrument mirrors. This deposit builds up in the range of 54 to 44 km,

corresponding to the middle and lower cloud layers (Fig. 1). The authors obtain the spectrum for the absorption due to the deposit. The SO_2 profile is determined via differential absorption with respect to 384 nm. Four thin absorbing layers were found by ISAV-2, three having exact counterparts seen with ISAV-1.

A list of the vertical features seen in these profiles is given in Table II.

3. Comparison with Previous SO_2 Measurements. In Table III we show a summary of previous measurements of SO_2 below 60 km. At an altitude of $z = 22$ km, the PV Large probe gas chromatograph and the Venera 12 lander gas chromatograph measured a concentration above 130 ppm: (130±35) ppm for Venera 12 (Gel'man et al. 1979) and (185±43) ppm for Pioneer Venus (Oyama et al. 1980, Table 2). At 22 km, the ISAV experiment obtains $n_{SO_2}(z) = 38$ ppm both for ISAV-1 and ISAV-2.

Table III also includes more recent measurements obtained from Earth through high-resolution spectroscopy of the infrared light emerging on the night side through the clouds of Venus (Bézard et al. 1993). They have interpreted their superb spectra to give a mixing ratio of 130±40 ppmv in the altitude range of 35 to 45 km, quite compatible with the ISAV-1 value of 125 ppmv at the peak of 42 km. The ISAV-1 average over the range 35 to 45 km is rather 90 to 100 ppmv, a value still compatible with Bézard et al. estimate.

The fact that ISAV SO_2 data are in good agreement with groundbased spectroscopy in the region 35 to 45 km gives some confidence in the SO_2 retrieval algorithm and also the optical thickness measurement in the whole range 10 to 60 km. Although Bertaux et al. consider that the low values measured in the lower atmosphere of Venus are real, the many assumptions in the analysis and thus the somewhat uncertain performance of the experiment in these most extreme Venus conditions may justify some skepticism.

The concentration of SO_2 (in cm^{-3}) is slowly increasing with decreasing altitudes, but the mixing ratio of SO_2 is decreasing. If this decline of SO_2 mixing ratio at lower altitudes is real, as advocated by Bertaux et al. (1996), it implies a large transport of SO_2 downward, with a flux of $\cong 4 \times 10^{13}$ mol $cm^{-2}s^{-1}$ at 40 km and $\cong 16 \times 10^{13}$ mol $cm^{-2}s^{-1}$ at 10 km. The measurements stop at 6 km altitude, but a reasonable extrapolation down to the surface shows that this downward flux might vanish on the surface. Therefore, it is not in contradiction with a reaction rate of SO_2 with calcite at the surface of the order of 5×10^{10} mol $cm^{-2}s^{-1}$ (see the chapter by Fegley et al.). On the other hand, the decrease of the downward flux of SO_2 with decreasing altitude would imply the chemical transformation of SO_2 to another sulfur bearing chemical species, whose production in the lower atmosphere (10–40 km) would provoke an upward flux equivalent to the SO_2 downward flux, which is so far undetected. Further, our present understanding of Venus thermal chemistry does not reproduce such a decline of SO_2 at low altitudes (see below, Sec. II).

TABLE II

Thickness and Boundary Altitudes of Various Regions from ISAV Observations[a]

	ISAV-1			ISAV-2		
	Upper Boundary	Lower Boundary	Thickness	Upper Boundary	Lower Boundary	Thickness
Region 1[b]	62.5	56.6	6.0	62.5	56.5	6.0
Upper cloud[c]	66	56	10			
Region 2	56.5	49.6	6.9	56.5	51	5.5
Middle cloud	56	50	6			
Region 3	49.6	41.3	8.3	51	43.1	7.9
Lower cloud	50	47	3			
Layer a				51.1	49.8	1.3
Layer b	49.5	47.0	1.5	49.8	47.8	2.0
Layer c	47.0	43.9	3.1	47.8	44.7	3.1
Layer d	43.8	41.0	2.8	44.7	43.1	1.6
Region 4	41.3	31.3	10	42	32.3	9.7
Event[d]	18.0	18.0	NA	NA	NA	NA
Region 5	31.3	0	31.3	32.3	0	32.3

[a] All altitudes and thicknesses are in km.
[b] Boundary altitudes of ISAV regions and absorbing layers are visually defined on the plotted lightcurves (Fig. 9).
[c] Boundaries of Venus clouds are quoted from the night probe of Pioneer Venus (Ragent and Blamont 1980).
[d] Altitude of mechanical event in ISAV-1 lightcurve.

TABLE III
Summary of SO_2 Measurements

Instrument, observations	12 km	22 km	42 km	52 km	Reference
					In-situ
PV Large probe gas chromatograph		185±43	>176	<600	Oyama et al. (1980)
PV Large probe mass spectrometer		<300		<10	Hoffman et al. (1980)
Venera 12 lander gas chromatograph		130±35			Gel'man et al. (1979)
ISAV active spectroscopy	25±2	38	125	150 (ISAV-1)	Bertaux et al. (1996)
					Earth-based
Infrared night spectra			130±40 (35–45 km)		Bézard et al. (1993)

II. CHEMISTRY OF VENUS' ATMOSPHERE

Venus' atmosphere can be divided into several regions with different chemical conditions. The lower atmosphere extends up to 60 km, and only solar radiation longer than the ultraviolet can reach this region. The middle atmosphere is located between 60 and 110 km. This region is under control of photochemistry. The upper atmosphere is above 110 km, and dissociation, ionization, and ionospheric reactions occur there. Neutral reactions are scarce in this upper region, and a variety of transport phenomena are of interest in chemical-dynamical modeling. This division is close to, though it does not exactly coincide with the division into troposphere, strato-mesosphere, and thermosphere. In what follows, we restrict our discussion to the two lower regions. The Venus thermosphere is discussed in the chapters by Fox et al. and by Bougher et al.

A. Lower Atmosphere (0–60 km)

1. Introduction. High temperature and pressure and the absence of effective photolysis processes are typical of this region. The atmosphere consists of stable components, and chemical reactions are very slow despite the high temperature and pressure. At first, we consider some tools to be used to study this region.

Thermochemical Equilibrium. The first studies for the lower atmospheric composition were based on the assumption of thermochemical equilibrium at each height (see, e.g., Florensky et al. 1978). This assumption is valid if the time to reach equilibrium (which may vary from minutes to millions of years) is less than the mixing time, which is of the order of a few years in this region. Krasnopolsky and Parshev (1979) argued that thermochemical equilibrium may be valid for most of species near the surface due to possible catalytic action of surface rocks, while constant mixing ratios better approximate the vertical density profiles at higher altitudes. Therefore, we recommend the equilibrium assumption either for processes which are known to be fast (e.g., $H_2SO_4 = H_2O + SO_3$) or for conditions near the surface of Venus. If measurements show a mixing ratio varying with height, then the local thermochemical equilibrium calculation may help to understand this variation.

Constancy of Element Mixing Ratio. A chemical element is conserved in chemical reactions, therefore its flux is constant throughout an atmosphere. Without condensation and below the homopause this flux is defined by

$$\phi_i = -K\left(\frac{dn}{dz} + \frac{n_i}{H_a}\right) = -Kn\frac{df_i}{dz}. \quad (2)$$

Here subscript i and a refer to the element and all atmospheric species, respectively, n is the number density, H is the scale height, f is the mixing ratio (fraction), K is the eddy diffusion coefficient. The flux may be neglected ($\phi_i \approx 0$), if $\phi_i \ll K n_i / H_a = K n_a f_i / H$. Therefore, f_i = constant if $f_i \gg \phi_i H_a/(K n_a)$, the element mixing ratio is constant with height. As an example, this rule is valid for elemental hydrogen below 45 km if its mixing ratio exceeds 2×10^{-11}, given the measured hydrogen escape flux of 7×10^6 $cm^{-2}s^{-1}$ (Rodriguez et al. 1984) and $K \approx 10^4$ cm^2s^{-1}. Therefore, to explain the water vapor mixing ratio decreasing from 200 ppm at 45 km to 20 ppm near 20 km, as proposed by Moroz et al. (1983), one should suggest another hydrogen-bearing component with mixing ratio $360/k$ ppm at 20 km. Here k is the number of hydrogen atoms in the molecule.

This rule is applicable to all elements on Venus below the cloud layer. However, it is exact only in a steady-state one-dimensional formulation. Advection and convection may break this rule, but typically not by very much. For example, to explain a wet location with f_{H_2O}>200 ppm below 20 km, a strong upward flow must be transported horizontally to form a downward flow at the observed site. This would presume that the measured profile of Moroz et al. (1993), is not typical, and the mean profile has f_{H_2O} constant with abundance 20 to 200 ppm below 20 km.

Local Instability. As discussed in Sec. II.A.1, local thermochemical equilibrium does not necessarily hold in the atmosphere, therefore thermochemically unstable species may exist. The best example is sulfuric acid which is thermochemically unstable on Venus. Its existence is explained because sulfuric acid is formed photochemically. Species formed photochemically or thermochemically may exist outside the region of formation if the transport time (mixing and precipitation) is shorter or comparable with the chemical destruction time. For example, H_2SO_4 is formed above 60 km and disappears below 40 km because loss processes are slower than transport between 60 and 40 km. Furthermore, the lifetime of a solution of $FeCl_3$ in concentrated sulfuric acid is close to one week at room temperature, but much longer between −20° and 0°C. Compared with the precipitation time of the mode 2 particles

(one month at 60–57 km), this helps to explain a coloration of the cloud layer at these heights by $FeCl_3$ (Zasova et al. 1981; Krasnopolsky 1985,1986), even though $FeCl_3$ is unstable in the presence of sulfuric acid.

2. Indirect Identifications of Aerosol Composition. Extensive experimental data on vertical profiles of aerosol particles, their multimodal distribution, the 300 to 500 nm absorption, its spectrum and location have resulted in many speculations about the aerosol chemical composition. Only sulfur has thermochemical plausibility as an aerosol material. Therefore, we come to the conclusion that the clouds must consist mostly of species of photochemical origin (e.g., H_2SO_4, Sn). In addition to H_2SO_4 which is indisputable, three candidates for the mode 3 (largest) particles have been considered: $HClO_4$, $AlCl_3$, and H_3PO_4 (see Krasnopolsky 1986,1989).

3. Sulfur Chemistry. This is clearly very important in the lower atmosphere of Venus. The chemical scheme proposed by Prinn (1975,1978,1979) is based on a prediction by Lewis (1970) of sulfur species with mixing ratios of 60 ppm for OCS, 6 ppm for H_2S, and 0.3 ppm for SO_2. In the 1970s, sulfuric acid was clearly identified in the clouds, while a search for gaseous sulfur components was not successful until 1979 (see Esposito et al. 1983). Prinn (1975) suggested a scheme of photochemical formation of sulfuric acid from carbonyl sulfide OCS and later (Prinn 1978) proposed the inverse processes leading to OCS and elemental sulfur from H_2SO_4:

$$SO_x + CO \longrightarrow SO_{x-1} + CO_2$$

$$\frac{S + CO + M \longrightarrow OCS + M}{\text{net } H_2SO_4 + 4CO \longrightarrow H2O + 3CO_2 + OCS.} \qquad (3)$$

The predicted SO_2 mixing ratio was of a few ppm above 30 km and much larger than that near the surface. Prinn (1979) supposed that dissociation of S_3 and S_4 by the near ultraviolet ($\lambda \approx 350$ nm) might produce hot sulfur atoms which could drive the chemistry.

Pioneer Venus, the Veneras, and groundbased observations showed that the main sulfur species is SO_2 with a mixing ratio close to 150 ppm, and that elemental sulfur in the vapor phase is an important absorber below 25 km. At these heights photons with $\lambda > 450$ to 500 nm are the only ones available, and the energy of sulfur atoms released by photolysis of S_3 and S_4 is too low to drive effectively the exothermic reactions. Later Prinn (1985; see also von Zahn et al. 1983) summarized the sulfur chemistry on Venus considering three sulfur cycles, one geological and two atmospheric (see Fig. 6 in the chapter by Fegley et al.).

Slow Atmospheric Cycle of Sulfur: Recent Results. The measured abundances and particularly the gradients of OCS and CO should be directly connected with the slow atmospheric cycle of sulfur and have been analyzed by Krasnopolsky and Pollack (1994). Their scheme is opposite to a certain extent to that of Prinn (1978); Prinn argued that SO_3 forms OCS, gradually

losing oxygen atoms in the reactions with CO, while Krasnopolsky and Pollack showed that SO_3 depletes OCS and CO below the clouds. Krasnopolsky and Pollack emphasize that this is only a partial solution to the problem of explaining the processes which govern profiles of OCS, CO, H_2SO_4, and SO_3, and their study does not cover some aspects of sulfur chemistry below 25 km, e.g., the reactions stimulated by the formation of SO. The main parameter of the model is the sulfuric acid column production rate $\phi_{H_2SO_4}$. Then, the H_2O mixing ratio below 30 km, f_{H_2O} (30 km), is chosen to fit the observed f_{H_2O} = 1 to 10 ppm at 62 to 65 km. Results of two models are given in Figs. 10 and 11 and in Table IV. The difference between the two models is that $\phi_{H_2SO_4}$ is equal to 2.2×10^{12} and 6.4×10^{12} $cm^{-2}s^{-1}$ in models 1 and 2, respectively. Then f_{H_2O} (30 km) = 30 ppm and 90 ppm. Therefore, model 1 fits the data of the nightside near-infrared spectroscopy, while model 2 is closer to the earlier interpretation of Venera 11–14 data for water vapor (Moroz et al. 1983). The required fluxes of CO are 1.7×10^{12} and 4.2×10^{12} $cm^{-2}s^{-1}$, respectively. As discussed in Sec. II.A.1, fluxes of sulfuric acid and CO are determined by the net processes of photochemistry above 58 km:

$$CO_2 + SO_2 + h\nu \longrightarrow CO + SO_3$$

$$3SO_2 + 2h\nu \longrightarrow 2SO_3 + S. \qquad (4)$$

Therefore, it is easy to determine a flux of elemental sulfur, if fluxes of H_2SO_4 and CO are known. This gives the sulfur to sulfuric acid mass flux ratios of 1:27 and 1:18 in models 1 and 2, respectively. The predicted mixing ratios of sulfuric acid vapor are equal to 5 ppm and 10 ppm near the lower cloud boundary. The latter fits better to the radio occultation studies with the Magellan spacecraft (Jenkins et al. 1994). Both models require the reaction rate coefficients

$$k_1 = 10^{-11} \exp(-(13100 \pm 1000)/T) \text{ cm}^3 \text{ s}^{-1}$$

$$k_2 = 10^{-11} \exp(-(8900 \pm 500)/T) \text{ cm}^3 \text{ s}^{-1} \qquad (5)$$

and the OCS mixing ratio near the surface f_{OCS} (0 km) = 28±1 ppm. The derived rate coefficients are in reasonable agreement with some analogs of the considered reactions. The OCS mixing ratio is close to 20 ppm and 5 to 30 ppm given by Krasnopolsky and Parshev (1979) and Fegley and Treiman (1992), respectively.

This approach does not cover all aspects of sulfur chemistry below Venus' cloud layer and the problem needs further study.

4. Processes in the Clouds: Position of the Sulfuric Acid Lower Cloud Boundary. Analysis of processes in Venus' clouds requires saturated water and sulfuric acid vapor pressures p_1 and p_2 as functions of temperature and concentration of the acid solution (Krasnopolsky and Pollack 1994). Using these relationships, Krasnopolsky and Pollack (1994) developed a method

TABLE IV

Comparison of Two Chemical Models for the Lower and Middle Atmosphere of Venus

Parameter	Model 1	Model 2
Photochemical analog	Yung and DeMore (1982) Model C	Krasnopolsky and Parshev (1981)
k(CICO cycle)	Supported by kinetic data	100 K (Model 1)
(O_2 abundance)/ (upper limit)	13	2.5
Production of H_2SO_4	$\approx 2 \times 10^{12} cm^{-2} s^{-1}$	$\approx 6 \times 10^{12} cm^{-2} s^{-1}$
S/H_2SO_4 in aerosol	(0–4)%	(6–15)%
f_{H2O} (30 km)	30 ppm (agrees with spectroscopy of nightside (Pollack et al. 1993)	90 ppm (close to Venera results (Moroz et al. 1983)
Lower boundary of H_2SO_4 aerosol	48.4 km (agrees with *in-situ* data)	46.5 km (agrees with radio occultation)
f_{H2SO4} (45–47 km)	5 ppm	10 ppm (close to radio occultation data (Jenkins et al. 1994)
H_2SO_4-Mode 3 extinction in the middle cloud layer	0.3 km^{-1}	0.9 km^{-1}
Mode 3 LCPS data corrected for high aspect crystals	≈ 1	Contradicts this hypothesis

to calculate the lower cloud boundary (henceforth LCB), for a given flux of H_2SO_4. LCB is at 48.4 km in model 1 (see above) and at 46.6 km in model 2. These values may be compared with measurements: nephelometers on four PV probes give 48.4±0.75 km (Ragent and Blamon 1980); nephelometers on five Venera probes 49.3±0.57 km (Marov et al. 1983); and photometric data of four Venera probes 48.7±0.45 km. The measurements favor model 1. However, the PV radio occultation observations (Cimino 1982) show the LCB varying from 47 to 48 km at the low and middle latitudes to 47 to 43 km at high and subpolar latitudes.

Variations of the Lower Cloud Layer. The LCB varies due to variations of the H_2SO_4 vapor mixing ratio, the water vapor mixing ratio below the clouds, and temperature and pressure. Krasnopolsky and Pollack (1994) found that variations of LCB are produced mostly by variations of the sulfuric acid abundance and temperature. Variations of density of the lower cloud layer reflect variations of gaseous sulfuric acid, because water contributes only

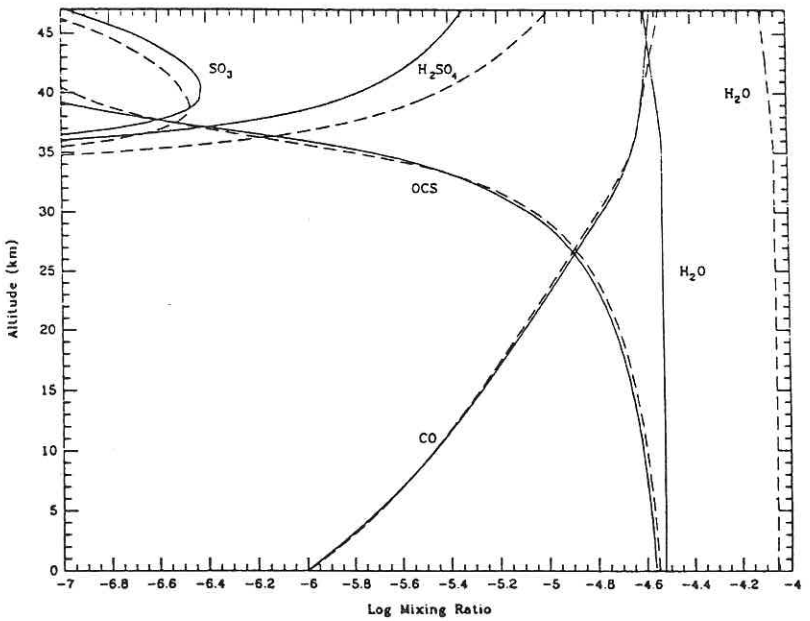

Figure 10. Mixing ratios for OCS, CO, SO_3, H_2SO_4 and H_2O in the lower atmosphere for models 1 (solid lines) and 2 (dashed line). For details, see text and Table IV (figure from Krasnopolsky and Pollack 1994).

slightly to the sulfuric acid aerosol in the lower cloud layer. Due to dynamics of the atmosphere at 60 to 70 km, more or less sulfur dioxide is exposed to solar radiation $\lambda < 219$ nm which transforms SO_2 to sulfuric acid, and more or less oxygen which affects this transformation may be available at different locations. Temperature variations are not very important in variations of density of the lower cloud layer; a temperature decrease of 6 K which lowers the LCB by 1 km, results in an increase of the cloud density by 13%.

Structure of the Cloud Layer. As discussed in the next section, photochemical models by Krasnopolsky and Parshev (1981*b*,1983) and Yung and DeMore (1982) show that sulfuric acid is produced mostly in a thin layer of 2 km depth centered at 62 km. Therefore, we model this layer by a Gaussian of this width, while the value of the integrated production, which is equal to the downward flux of H_2SO_4 below 60 km, $\phi_{H_2SO_4}$, is the main parameter for modeling the cloud layer and chemistry of the atmosphere below the clouds (see above).

Krasnopolsky and Pollack (1994) proved that the flux and concentration of liquid sulfuric acid and mixing ratios of H_2O and H_2SO_4 vapors are

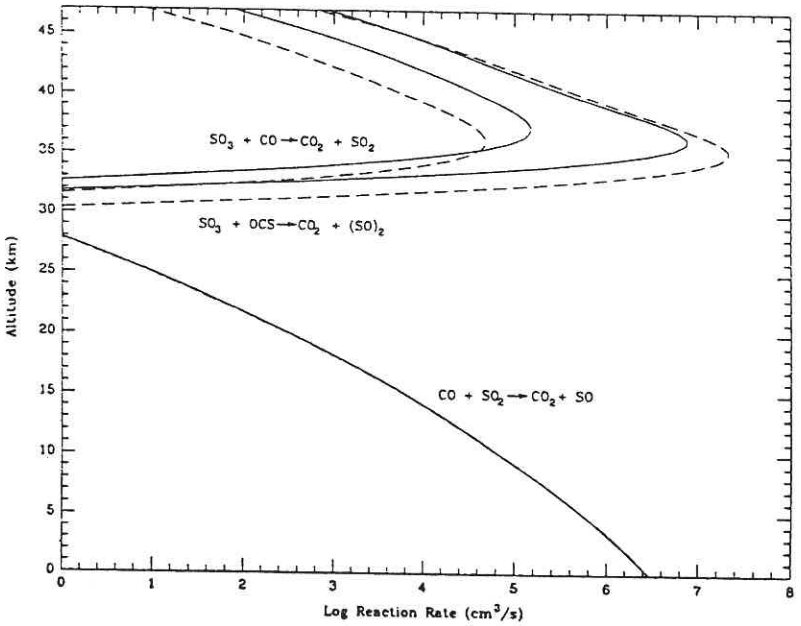

Figure 11. Reaction rates for model 1 (solid lines) and model 2 (dashed lines) from Krasnopolsky and Pollack (1994).

connected by equation

$$\phi_1 = \frac{K[CO_2]}{1+m}\left(\frac{df}{dz} - m\frac{df_1}{dz}\right) \tag{6}$$

for the single unknown $m(z) = H_2O/H_2SO_4$ in liquid sulfuric acid. This value is equivalent to concentration and more convenient, because chemical potentials μ_1 and μ_2 are given in Giauque et al. (1960) as function of m. If $m(z)$ is known, then $f_1(z)$ and $f_2(z)$ are also known, therefore $m(z)$ is really the only unknown in this equation (which is valid only above the LCB).

To solve this equation, one needs the sulfuric acid flux (ϕ_1 in this formulation), its mixing ratio at LCB, and the H_2O mixing ratio at LCB. The H_2SO_4 mixing ratio as function of ϕ_1 was discussed in Sec. II.A.3, and is determined by chemical processes in the atmosphere below the clouds. A choice of the H_2O mixing ratio below the clouds is determined by spectroscopic observations (Fink et al. 1972; Barker 1975) which give $f_{H_2O} = 1$ to 10 ppm at 62 to 65 km. The calculated structure of the cloud layer for models 1 and 2 ($\phi_{H_2SO_4} = 2.2 \times 10^{12}$ and 6.4×10^{12} $cm^{-2}s^{-1}$, respectively) is shown in Fig. 12.

Considering the flux of sulfuric acid droplets, it is possible to divide the clouds into three layers. Due to the photochemical formation of sulfuric acid,

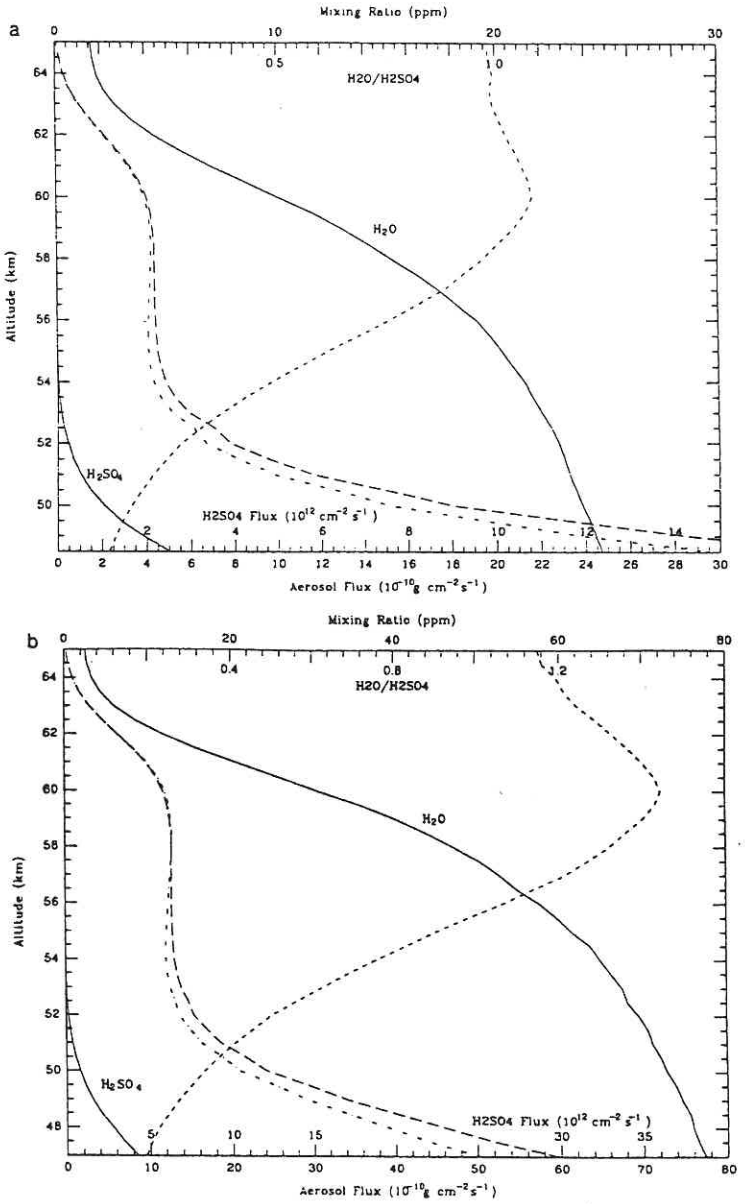

Figure 12. Calculated results for vertical distribution of H_2O and H_2SO_4 in the cloud layer from Krasnopolsky and Pollack (1994). Solid lines: mixing ratios. Short-dashed curves: H_2O/H_2SO_4 ratio in the cloud particles. Long-dashed curve: downward flux of liquid phase H_2SO_4. Dash-dotted curve: downward flux of sulfuric acid droplets. Panel a: model 1; panel b: model 2. See Table IV and text.

its flux increases steeply in the upper cloud layer which ends near 59 km (the measurements give 57 km). This increase correlates with the increasing H_2O mixing ratio while m and concentration of sulfuric acid is relatively constant at 84% and 81% in models 1 and 2, respectively. Measurements show 75 to 85% (Pollack et al. 1978; Reed et al. 1978) and agree with these models.

The flux of liquid sulfuric acid is constant in the middle cloud layer at 59 to 52 km (57–50 km according to the measurements). The increase of f_{H_2O} is only by a factor of 1.5, while m decreases from the top to the bottom of the middle cloud layer by a factor of 3 to 4. This variation changes the concentration from 81 to 84% to 93 to 94%.

In the lower cloud layer at 52 to 48 km, the flux of liquid sulfuric acid exceeds that in the middle cloud layer by a factor of 4 to 7. The H_2O mixing ratio is rather constant, and m continues to decrease by a factor of 3 until the LCB is reached. This corresponds to the concentration increasing to 97 to 98% at the LCB. The important feature of the lower cloud layer is the decrease of sulfuric acid vapor from 5 to 10 ppm at LCB to $\approx$0.5 ppm at the top of the lower cloud layer. A strong gradient of gaseous sulfuric acid drives this upward flux which condenses and forms a strong downward flux of liquid sulfuric acid with the sum of both fluxes being constant in the lower and middle cloud layers. This is the mechanism of formation of the lower cloud layer.

Comparison of the Models with Measurements. For the middle cloud layer, the nephelometric measurements and the photometric measurements show a spread of 20% between the data of the various probes. This shows it is stable around the planet; the conclusion is confirmed by the small horizontal variations seen by the Vega balloons. Therefore, Krasnopolsky and Parshev compare their models to the PV LCPS data (see Fig. 1).

The aerosol flux precipitating at the Stokes velocity is given by

$$\phi = \frac{8\pi}{27}\frac{g\rho^2 r^5}{\eta} n. \tag{7}$$

Coupling the values of the flux with the relationships for the flux and extinction coefficient, one can find the mode 3 extinction coefficient is 0.3 km^{-1} and 0.9 km^{-1} for models 1 and 2, respectively. Then model 1 means that either H_2SO_4 is the only species of the Mode 3 particles (if the interpretation in Esposito et al. [1993] is preferable) or it constitutes a third of large particle material (if the initial LCPS data are adopted), the rest may be $AlCl_3$ or other species (see Sec. II.A.2). Model 2 favors the initial LCPS data and sulfuric acid as a main component of the middle cloud layer. We prefer model 1 because it corresponds to the recent measurements of 30 ppm of H_2O below 30 km, though this model fits worse than model 2 to the sulfuric acid vapor mixing ratio at LCB.

B. Photochemistry from 60 to 110 km

1. Early Models. Actually, the period of intense studies of Venus' photochemistry was rather short and lasted from 1971 to 1982. Papers published before 1971 are of comparatively low interest, and there are no original publications on the subject in the last thirteen years. Another interesting and important aspect of the problem (mentioned by Prinn 1985) is that studies of chlorine and sulfur chemistry in and above Venus' clouds preceded a discovery of the importance of the similar processes in the Earth's atmosphere. This case shows a direct impact from planetary atmospheres studies for understanding phenomena in our own atmosphere.

2. Post-Pioneer Venus Models. Among the many new atmospheric results from Pioneer Venus and the Venera 11 and 12 probes, the most important facts for photochemistry were (1) SO_2 is the main sulfur-bearing species with the mixing ratio of 150 ppm in the lower atmosphere; (2) H_2O has a mixing ratio of 200 ppm near the lower cloud boundary (which is now thought to be 25 ppm—see model 1 in Sec. II.A.3); (3) a steep decrease of the SO_2 mixing ratio with altitude to 100 ppb at the 40 mbar level (69 km) where the SO_2 scale height was equal to 1 km (later results showed a continuous decline with time of SO_2 at this level from 100 ppb to 20 ppb and scale height in the range 2 to 3 km; more recently the abundances were corrected to be larger by a factor of 4; the currently accepted values are 100 ppb and 3 km for the period of 1982 to 1992; see Fig. 5); and (4) data for O, CO, H, and N in the upper atmosphere. Photochemical papers published soon after (Winick and Stewart 1980; Krasnopolsky and Parshev 1980,1981*a,b*,1983) reflected these findings.

Winick and Stewart (1980) modeled photochemistry of HO_x, ClO_x, SO_x, and O_x between 58 and 96 km, thus combining chlorine and sulfur chemistries. Their kinetic data were substantially improved compared with Prinn (1975) and Sze and McElroy (1975) due to five years of progress in the field. For example, the reactions of ClO and ClOO with CO were known as extremely slow and unimportant at that time. Formation of CO_2 via the reaction CO + OH is not effective, and the total production of sulfuric acid is smaller by a factor of 30 than the column CO_2 photolysis in that model. Almost all CO and O_2 formed by the CO_2 photolysis does not recombine to CO_2, and they are thus transported downward to the lower atmosphere. The spectroscopic limit of $f_{O_2}<0.3$ ppm or the O_2 column abundance $N(O_2)<1.5 \times 10^{18}$ cm^{-2} at 62 km (Trauger and Lunine 1983) is exceeded by a factor of 150 in this model. However, at that time contradictory data on O_2 from the PV gas chromatograph prevented the proper understanding of the O_2 problem. The H_2O mixing ratio was fixed at 1 ppm throughout the atmosphere, and the SO_2 abundance of 4 ppm was chosen at 58 km as a parameter to fit the measured SO_2 mixing ratio at 70 km.

Krasnopolsky and Parshev (1981*a,b*,1983) developed a model for the altitude range from 50 to 200 km. To a certain extent this is the most complete model of Venus' photochemistry, because it considers together the problems of formation of sulfuric acid, its concentration, and vertical profiles of H_2O and SO_2; further, this is without the simplifying assumptions of $f_{H_2O} = 1$ ppm

throughout the atmosphere and of SO_2 at the lower boundary as a fitting parameter. However, the kinetic data used in the model are from compilations by Kondratiev (1971) and Baulch et al. (1976) and are poor compared to those used in Winick and Stewart (1980) and especially in Yung and DeMore (1982). A very important cycle which is currently thought to be responsible for recombination of CO and O_2 to CO_2 on Venus was suggested in that paper:

$$\begin{aligned} &\mathrm{CO + Cl + } M \longrightarrow \mathrm{ClCO + } M \qquad k_1 \\ &\mathrm{ClCO + } M \longrightarrow \mathrm{CO + Cl + } M \qquad k_2 \\ &\mathrm{ClCO + O_2} \longrightarrow \mathrm{CO_2 + ClO} \qquad k_3 \\ &\overline{\text{net } \mathrm{CO + O_2 + Cl} \longrightarrow \mathrm{CO_2 + ClO.}} \end{aligned} \tag{8}$$

ClO reacts with either O to form O_2 or SO to form SO_2. The collisional decomposition of ClCO was underestimated by Krasnopolsky and Parshev by 2 orders of magnitude due to a misprint in Kondratiev (1971). Therefore the effective rate coefficient of the cycle $k = k_1k_3/k_2$ appears to be overestimated by two orders of magnitude. Another cycle suggested is

$$\begin{aligned} &\mathrm{CO + Cl + } M \longrightarrow \mathrm{ClCO + } M \\ &\overline{\mathrm{ClCO + O} \longrightarrow \mathrm{CO_2 + Cl}} \\ &\overline{\text{net } \mathrm{CO + O} \longrightarrow \mathrm{CO_2.}} \end{aligned} \tag{9}$$

Due to the fact that the model of Yung and DeMore overestimates the O_2 abundance using the more realistic cycle efficiency by a factor of 10, the Krasnopolsky and Parshev model which gives the extreme case is of some interest, because it overpredicts oxygen by only a factor of 2.5. In the model, all atomic oxygen produced by photolysis of CO_2 above this height recombines to form O_2. Below 87 km, a strong sink for both O_2 molecules moving downward and those newly formed at these heights is due to the ClCO cycle. The O_2 column density is under control of eddy diffusion and is equal to 3.7×10^{18} cm^{-2} which was less than the upper limit of 5×10^{18} cm^{-2} that existed at that time (Traub and Carleton 1974). To fit the current upper limit of 1.5×10^{18} cm^{-2}, the eddy diffusion coefficient at 80 to 90 km should be equal to 10^6 cm^{2}s^{-1}, i.e., larger by a factor of 3 than that used in the model. Oxygen is so scarce at 60 to 65 km, that oxidation of SO_2 to SO_3 with further formation of sulfuric acid must take oxygen also from SO_2 to form sulfur aerosols. The number of photons in the range of 202 to 219 nm which dissociate SO_2 is equal to 1.5×10^{13} cm^{-2}s^{-1} for global-mean conditions; therefore, the full production of sulfuric acid is close to 5×10^{12} cm^{-2}s^{-1}. Sulfuric acid and sulfur aerosols are formed with a mass ratio 7.3:1. Photolysis of SO_2 occurs in a thin layer centered at the altitude where the slant optical depth for SO_2 absorption is unity.

This corresponds to 64 km for the measured mixing ratio of 10^{-7} at 69 km using current SO_2 data (Zasova et al. 1993; Na et al. 1994) which differ from

those used by Krasnopolsky and Parshev. The SO_2 flux is constant up to the thin layer centered at 64 km and is equal to $\phi_0 = 7.5 \times 10^{12}$ cm^{-2}s^{-1} (see equation in Sec. I.2).

This gives $f_{SO_2} = 80$ ppm at 50 km which may be compared with 50 ppm at this height from the photometry at the Venera 14 descent probe (Ekonomov et al. 1983). Each SO_3 molecule captures two H_2O molecules forming 85% sulfuric acid. Therefore the fact that the H_2O mixing ratio at 64 km is much smaller than that at 50 km, requires f_{H_2O} (50 km) $\approx f_{SO_2}$ (50 km) $\times 4/3 = 110$ ppm. We see that this model correlates with model 2 considered in Sec. II.A where the H_2SO_4 flux was equal to 6.4×10^{12} cm^{-2}s^{-1} and $f_{H_2O} = 75$ ppm at 50 km.

3. Models by Yung and DeMore (1982). These models give the most comprehensive study of the photochemistry in the altitude region 58 to 110 km. Their important advantage is a very healthy kinetic data set. Though the models are thirteen years old now, we have not found that later studies of chemical processes relevant to these models significantly affect their results. Similar to Winick and Stewart (1980), Yung and DeMore do not consider the water vapor profile (assuming constant $f_{H_2O} = 1$ ppm) and concentration of sulfuric acid aerosol, and use the SO_2 mixing ratio at the lower boundary of 58 km as a fitting parameter to match their models with the SO_2 observations available at that time.

As discussed above, the central problem of Venus' photochemistry is the low abundance of O_2 above the clouds. Hydrogen, chlorine, and sulfur chemistries are each involved in the fate of the CO_2 photolysis products. The main source of active hydrogen and chlorine species (henceforth H* and Cl*) is photolysis of HCl. Though H* and Cl* production rates are equal and their losses are equal as well, due to the reactions

$$\begin{aligned} &\mathrm{Cl + HO_2} \longrightarrow \mathrm{HCl + O_2} \\ &\mathrm{H + Cl_2} \longrightarrow \mathrm{HCl + Cl} \end{aligned} \tag{10}$$

their densities may be quite different because of the reactions (Krasnopolsky 1986)

$$\begin{aligned} &\mathrm{OH + HCl} \longrightarrow \mathrm{H_2O + Cl} \\ &\mathrm{H + HCl} \longrightarrow \mathrm{H_2 + Cl} \\ &\mathrm{Cl + H_2} \longrightarrow \mathrm{HCl + H.} \end{aligned} \tag{11}$$

The first two reactions transform H* to Cl*, and the third reaction vise versa. Their column rates are balanced, and thus we have

$$\frac{[\mathrm{H^*}]}{[\mathrm{Cl^*}]} \approx 0.1 \frac{[\mathrm{H_2}]}{[\mathrm{HCl}]}. \tag{12}$$

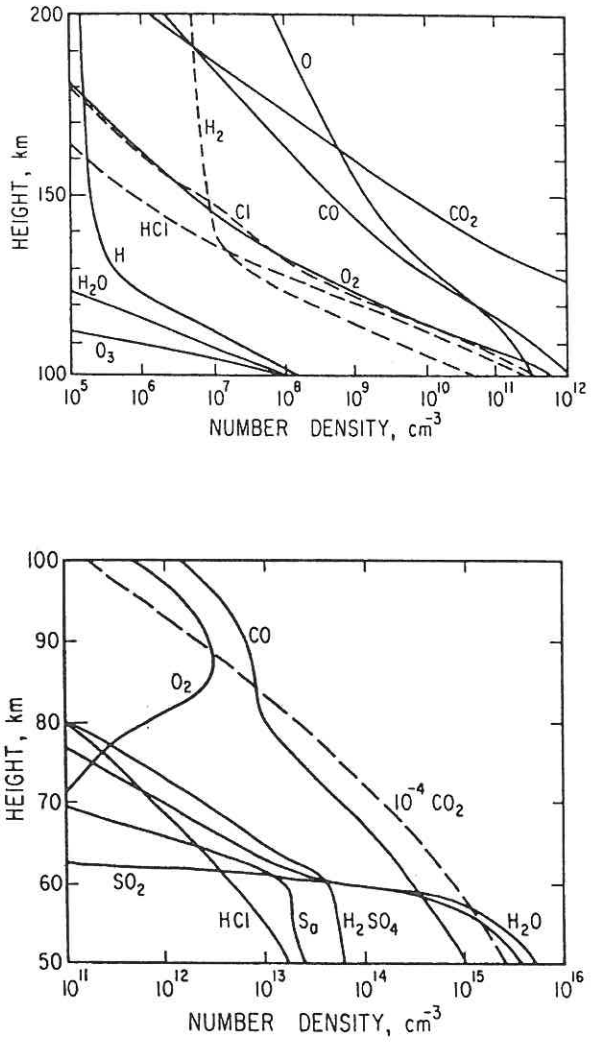

Figure 13. Chemical composition of Venus atmosphere from Yung and DeMore (1982) model C.

Here 0.1 is the ratio of the rate coefficients for a mean temperature of 230 K. Therefore relative importance of the H* and Cl* cycles depends strongly on the H_2 abundance which was rather uncertain.

Model A is based on the suggestion by Kumar et al. (1991) that ions of a mass number 2 measured by the PV ion mass spectrometer were H_2^+. We do not consider this model viable, because the mass 2 ions are currently recognized to be D^+ (McElroy et al. 1982) which requires the D/H ratio of

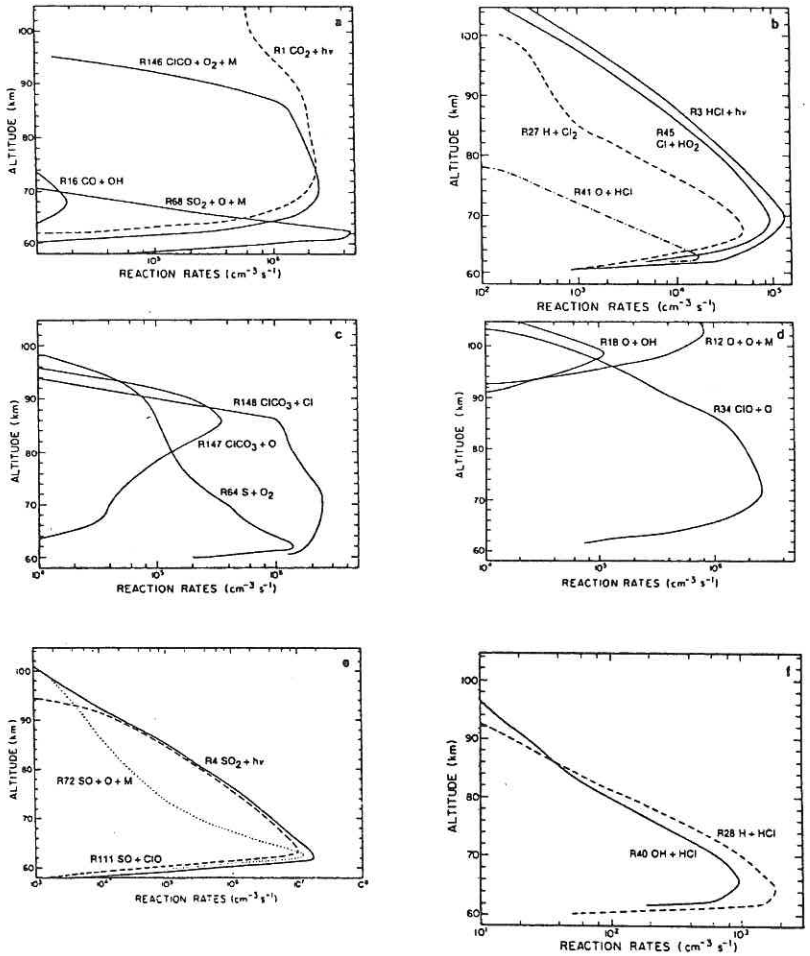

Figure 14. Results from Yung and Demore (1982). Model C: (a) sources and sinks of free oxygen; (b) HO_x and ClO_x; (c,d) formation of O_2; (e) equilibrium between SO_2 and SO; (f) production rates for H_2 and H_2O.

10^{-2} (see the chapter by Donahue et al.). Later, an upper limit of f_{H_2}<0.1 ppm was established from those measurements (Kumar and Taylor 1985).

Model B adopts f_{H_2} = 0.5 ppm which is still higher than the upper limit. This model is likewise not viable. Model C assumes that all H_2 molecules in the atmosphere above the lower boundary at 58 km are produced photochemically. Except for the CO_2 and H_2O profiles, the model includes conditions at the lower boundary: f_{CO} = 45 ppm, f_{SO_2} = 4 ppm (free parameter), f_{HCl} = 0.8 ppm (twice the measured value); velocities of O_2, Cl_2, H_2, and O;

$v = -0.6$ K/H $= -0.02$ cm s^{-1}; and photochemical equilibrium for other species. Downward fluxes of 10^{12} cm^{-2}s^{-1} (which are equal to the column photolysis rate of CO_2 above 110 km) are taken for CO and O at 110 km. Fluxes of other species are assumed to be zero at the upper boundary. The results of calculations are shown in Figs. 13 and 14. The main cycles which determine balance of CO, O_2, and O are those with ClCO (see the previous section). Rates of the key reactions of these cycles are shown in Fig. 14. The O+O+M and O+OH reactions add to production of O_2, and the reaction S+O_2 reduces slightly its abundance which is equal to 1.8×10^{19} cm^{-2}, and thus exceeds the upper limit by an order of magnitude. The balance of H* and Cl* and formation of H_2O and H_2 are also shown in Fig. 14. Photolysis of CO_2 having the column rate of 7.6×10^{12} cm^{-2}s^{-1} is not completely balanced by production of CO_2, and therefore some fraction of the total production of CO equal to 1.4×10^{12} cm^{-2}s^{-1} moves down to the lower atmosphere. The SO_2 mixing ratio is equal to 32 ppb at 70 km, and the SO_2 scale height is 2.5 km. Both values agree with the measurements. SO_2/SO = 25 at 70 km which is slightly larger than 10 from the measurements (Na 1992). Production and loss of SO are shown in Fig. 14e. Formation of sulfuric acid and its downward flux is equal to that of CO, and the net result of photochemistry is

$$CO_2 + SO_2 \longrightarrow CO + SO_3. \tag{13}$$

The downward flux of Cl_2 is smaller than those for CO and sulfuric acid by three orders of magnitude and equals 3×10^9 cm^{-2}s^{-1}. It is formed by the net process

$$2HCl + CO_2 \longrightarrow H_2O + CO + Cl_2. \tag{14}$$

The calculated Cl_2 mixing ratio is equal to 25 ppb near 58 km which is much smaller than 1 ppm of Cl_2 required to produce the 320 to 500 nm absorption (Pollack et al. 1980).

One of the photochemical problems is to explain a very intense airglow of $O_2(^1\Delta)$ at 1.27 μm with intensities of 1.2 MR and 1.5 MR on the night and day sides, respectively (Connes et al. 1979; see the chapter by Lellouch et al.).

Chlorine-SO_2 Interaction. This possibility is discussed by DeMore et al. (1985) and has two important aspects. The first one is the formation of sulfuryl chloride SO_2Cl_2 via

$$\begin{gathered} 2[Cl + SO_2 + M \longrightarrow ClSO_2 + M] \\ \underline{2ClSO_2 \longrightarrow SO_2Cl_2 + SO_2} \\ \text{net } 2Cl + SO_2 \longrightarrow SO_2Cl_2. \end{gathered} \tag{15}$$

DeMore et al. claimed that SO_2Cl_2 should be the most abundant chlorine species in the mesosphere with the expected mixing ratio of 4 ppm. The second one is enhanced removal of O_2 and formation of sulfuric acid:

$$Cl + SO_2 + M \longrightarrow ClSO_2 + M$$

$$\begin{gathered} ClSO_2 + O_2 + M \longrightarrow ClSO_4 + M \\ ClSO_4 + Cl \longrightarrow +SO_3 + ClO \\ SO_2 + h\nu \longrightarrow SO + O \\ ClO + SO \longrightarrow SO_2 + Cl \\ \underline{SO_2 + O + M \longrightarrow SO_3 + M} \\ \text{net } O_2 + 2SO_2 \longrightarrow 2SO_3. \end{gathered} \tag{16}$$

They suggest that a model with 4 ppm of SO_2Cl_2 and 0.4 ppm of HCl at the lower boundary might fit much better the experimental results than the models of Yung and DeMore (1982). However, this model has not been further developed. On the other hand, Pollack et al. (1993) concluded from the observed constancy of the HCl mixing ratio from the cloud tops to the surface that other chlorine species may be present in the atmosphere only with mixing ratios smaller than $\approx$0.2 ppm, therefore precluding 4 ppm of SO_2Cl_2. The chlorine-sulfur interaction is a promising way to explain the very low abundance of molecular oxygen and should be considered carefully in further improvements of Venus' photochemistry modeling.

Summary of the Models. There are some parallels between model 1 (low H_2SO_4) and model 2 (higher H_2SO_4 flux) for the lower atmosphere (Sec. II.A.) and the photochemical models of Yung and DeMore (1982) and Krasnopolsky and Parshev (1981*b*), respectively. Models 1 and 2 are determined by the column production rate (i.e., the downward flux) of H_2SO_4 which is equal to 2.2×10^{12} and 6.4×10^{12} cm^{-2}s^{-1}, respectively. The photochemical models respectively produce values of H_2SO_4 production close to these inputs. Comparison of the models is shown in Table IV.

We prefer model 1 because it is based on good kinetic data and agrees with the recent spectroscopic measurements of water vapor and with the position of the lower boundary of sulfuric acid in the clouds. Advantages of model 2 are: (1) the much smaller abundance of O_2; (2) presence of sulfur aerosol which is supported by measurements; (3) support by radio occultation measurements of the lower cloud layer (Cimino 1982), although Jenkins (1992) reprocessed these data and found no detection of cloud material; (4) sulfuric acid vapor mixing ratio (Jenkins et al. 1994); and (5) by water vapor spectroscopic measurements from the Venera probes. Further experimental and photochemical studies are needed. Clearly, chlorine-sulfur interactions will be a promising field for further development of Venus' photochemistry.

III. OPEN QUESTIONS AND FUTURE WORK

A. Unidentified Ultraviolet and Blue Absorption

Currently, the only positively identified absorbing species in the visible atmosphere are SO_2 and SO. However, they do not absorb longward of 3200 Å. Thus, other absorbers must explain the absorption in the Venus spectrum and dark markings that extend to 5000 Å (Esposito 1980; Pollack et al. 1980).

In addition, these other absorbers must explain the phase angle dependence of the ultraviolet dark markings (Barker et al. 1975) as well as their short lifetime above the clouds (from hours to days; see Esposito et al. 1983). This must also be consistent with the solar flux observations of Tomasko et al. (1980) which show absorption at 58 to 62 km, and little absorption below. Similar solar flux absorption results from Venera 14 (Ekonomov et al. 1983,1984) provide an additional constraint. Esposito and Travis (1982) noted the correlation between dark markings seen longward of 3200 Å and SO_2 enhancements seen at 2070 Å. Beyond the absorption spectrum, a good candidate must also match the vertical distribution, lifetime and correlation with SO_2 enhancement. This last correlation could be either chemical or dynamical, because the SO_2 visible in the far ultraviolet is likely the result of local upwelling (Esposito and Travis 1982). We briefly review the suggested candidates.

S_8. Hapke and Nelson (1975) and Young (1977,1983) proposed S_8 as the second absorber because it absorbs strongly in the ultraviolet. However, Pollack et al. (1980) showed that the spectral characteristics of S_8 were inconsistent with that of the second absorber. Another shortcoming of S_8 as the second absorber is its vertical profile. S_8 is not expected to disappear rapidly below the upper cloud layer because it precipitates as a solid, and the idea of these particles hiding inside sulfuric acid aerosols has been discounted by Young (1983). Thus, the vertical profile of S_8 does not match that of the second absorber. Furthermore, the chemical lifetime of S_8 above the clouds is much longer than the time scale of the dark markings, thus it is difficult to explain the rapid disappearance (lifetime <3 hr) of small scale dark markings (see, e.g., Rossow et al. 1980).

S_3 *and* S_4. Toon et al. (1982) suggested metastable sulfur allotropes, S_3 and S_4, as the most likely candidate for the second absorber. The absorption cross sections of S_3 peak around 400 nm and S_4, around 520 nm. The combination of these two sulfur gases with SO_2 provides a very close match to the albedo of Venus. The peak in the absorption cross sections of S_3 around 400 nm lines up with a kink in the albedo spectrum of Venus. S_3 and S_4 are metastable, and once produced they quickly relax to S_8 which exists as particulates. S_8 particles could then become incorporated into the sulfuric acid aerosols and fall out of the cloud region. This scenario thus explains the short lifetime of the dark features and the absence of the second absorber below the upper clouds. Furthermore, these sulfur allotropes can account for the high real refractive index of the upper cloud material, and the bimodal size distribution observed in the Venus clouds.

The production of sulfur allotropes may happen in oxygen poor areas in the atmosphere of Venus. With little oxygen in the atmosphere, sulfur allotropes are produced from SO_2 photolysis instead of sulfuric acid (Prinn 1975,1985).

Elemental sulfur can form photochemically from SO_2 if the efficiency of photochemical cycles which restore CO_2 from CO and O_2 is high. Then

formation of sulfuric acid may result from

$$3SO_2 + 2h\nu \longrightarrow 2SO_3 + S \tag{17}$$

and a mass ratio of productions of $H_2SO_4 \cdot H_2O$ to S is seven. However, if the efficiency is low, then sulfuric acid forms via

$$CO_2 + SO_2 + h\nu \longrightarrow CO + SO_3 \tag{18}$$

without elemental sulfur production (see Sec. II.B). S_3 and S_4 may be produced in areas where sulfur vapor is enriched. However, there have been no positive detection of S_3 or S_4 to date. Further, these allotropes are rapidly photodissociated, giving lifetimes close to 1 s in the upper cloud.

One major problem with the above scenario is that sulfur particles would still absorb ultraviolet photons below the upper clouds.

S_2O. Hapke and Graham (1985,1989) proposed that the disulfur monoxide (S_2O) and polysulfur oxides may be responsible for the ultraviolet markings in the clouds of Venus. They measured the relative reflectance of S_2O frost at 77 K, and found that it has low reflectivity in the wavelength region from 200 to 500 nm. Na and Esposito (1995) estimate the the chemical lifetime and vertical distribution of S_2O, both of which match the second absorber. Its obvious chemical connection with SO_2 could explain the correlations of the dark markings with SO_2 enhancements. Unfortunately, we do not have a good spectrum measured for the gas phase.

$FeCl_3$. Krasnopolsky (1985,1986) showed that many properties of the clouds can be explained if condensation of Fe_2Cl_6 occurs at 47.5 km at the PV sounder probe site. This means that this species mixing ratio is equal to 15 ppbv below 47.5 km. The calculated profile of the $FeCl_3$ condensate coincides with that of the mode 1 particles in the lower and middle cloud layer. The mode 1 $FeCl_3$ particles are transported by eddy diffusion to the upper cloud layer where they serve as condensation centers for the mode 2 H_2SO_4 particles. These particles are liquid below 62 to 63 km, and the $FeCl_3$ flux to the H_2SO_4 production rate ratio corresponds to a solution with concentration of $FeCl_3$ close to 1%. It is this solution which can explain the 320 to 500 nm absorption (Zasova et al. 1981). The reaction between $FeCl_3$ and concentrated H_2SO_4 is rather slow at temperatures 250 to 280 K at 62 to 58 km, and the lifetime of the solution is close to the precipitation time of one month. Colorless ferric sulfate replaces $FeCl_3$ near 58 km. Thermochemical equilibrium is

$$Fe_s(SO_4)_3 + 6HCl + 3CO = Fe_2Cl_6 + 3H_2O + 3SO_2 + 3CO_2. \tag{19}$$

Thus, elemental sulfur, S_2O, and ferric chloride solution in sulfuric acid are good candidate species responsible for the observed absorption at 320 to 500 nm, perhaps even in combination.

B. The Mode 3 Controversy

The LCPS measurement of mode 3 particles has provided a controversy that is still unresolved (see Esposito et al. 1983). The starting point for the mode 3 controversy comes from direct evidence for asymmetric (possible crystalline) particles provided by Knollenberg and Hunten (1980). Knollenberg et al. (1980) further state that only such crystals of high aspect ratio could satisfy the Pioneer Venus LCPS, LSFR, and LN results simultaneously. However, because the largest amount of mass (~80% according to Knollenberg and Hunten [1980]) is within the mode 3 particles, it is extremely important to verify their existence and determine their composition.

The LCPS undoubtedly detected large particles, but the evidence for solid particles is indirect. There were internal inconsistencies in the LCPS measurements as well as inconsistencies between the LCPS measurements and the measurements made by other instruments. Some of these inconsistencies were:

1. Calculations employing LCPS size distributions do not give the backscatter observed by the PV nephelometer in the lower clouds if reasonable refractive indices are used.
2. The LCPS size distributions do not yield the optical depths derived by the LSFR, assuming spherical particles.
3. Overlapping size ranges of the LCPS give conflicting measurements in the lower clouds.

In addition, independent Venera results show some oddities at the same altitudes: (1) Venera nephelometer phase function measurements are inconsistent with spherical particles having reasonable refractive indices in the lower cloud; (2) X-ray fluorescence measurements (Surkov et al. 1979) show about ten times as much chlorine as sulfur in the Venus clouds. The various inconsistencies can be explained by the simple hypothesis that mode 3 is composed of solid, nonspherical particles. However, this explanation requires an abundant gas-phase chemical in the clouds as the source for these particles. No such gas has yet been discovered.

Toon et al. (1982) reexamined the evidence that solid particles form a distinctive size mode. They find that mode 3 is defined by a discontinuity located between two size ranges of the LCPS. Although this could be real, it could also be the result of a small calibration shift of the PV instrument. A shift in the calibration removes the discontinuity, along with the internal inconsistency of the LCPS. The revised size spectrum is consistent with the Venera and Pioneer optical data in the lower clouds; all the modes can be composed of sulfuric acid droplets without any solid particles. The only unexplained data are those showing large amounts of chlorine compared to sulfur in the clouds. We note, though, that the more recent Soviet measurements from Veneras 13 and 14 show a large sulfur to chlorine ratio, the opposite of findings by Surkov et al. (1981). The Vega landers detected no large particles (see Sec. I.A.).

From the data in hand, it seems impossible to disprove the existence of mode 3. Two self-consistent, alternative interpretations of the data exist. Accepting the spacecraft observation at face value, we are led to the existence of a mode of large solid particles whose composition is unknown and whose source vapor has escaped detection. On the other hand, we may conclude that the large particle mode is merely the (mis-measured) tail end of the Mode 2 sulfuric acid droplets. This allows a simple understanding of the source of all the cloud particles, but at the cost of disbelieving some of the measurements.

C. Future Work

To advance our understanding of Venus chemistry, we require:

1. Better measurements of composition, including vertical and horizontal variation. Key species include SO_2, SO, H_2S, Cl_2, COS, and H_2O.
2. Better measurements of the cloud particle properties and their variation. The size distribution, shape and composition of the majority of the aerosol mass are still open, despite our assurance that "mode 2" (the aerosols visible at the cloud tops) are spherical droplets of concentrated sulfuric acid.
3. Determination of the rate and importance of surface–atmosphere interactions (see the chapter by Fegley et al.).
4. Detailed comparison of *in-situ* and remote determinations of water abundance in the deep atmosphere (see chapter by Taylor et al.).

This new information could justify more detailed models of the chlorine and sulfur cycles important in the atmosphere, and studies of the many interactions between radiation, clouds, chemistry and dynamics.

Acknowlegments. Esposito and Krasnopolsky acknowlege support from the Venus Data Analysis Program (VDAP). Moroz and Zasov acknowlege grants from the International Science Foundation Grants and the Russian Fundamental Science Foundation. We are grateful for careful reading of the manuscript by C. Na and P. Steffes.

REFERENCES

Allen, D. A., and Crawford, J. W. 1984. Cloud structure on the dark side of Venus. *Nature* 307:222–224.

Allen, D. A., Crisp, D., and Meadows, V. 1992. Variable oxygen airglow on Venus as a probe of atmospheric dynamics. *Nature* 359:516–519.

Andreychikov, B. M. 1987. Chemical composition and structure of the clouds of Venus inferred from the results of X-ray fluorescent analysis on descent probes VEGA 1 and 2. *Kosmich. Issled.* 25:737–743 (in Russian).

Andreychikov, B. M., et al. 1987. X-ray radiometric analysis of the cloud aerosol of Venus by the Vega 1 and 2 probes. *Kosmich. Issled.* 25:721–736 (in Russian).
Barin, I. 1989. *Thermochemical Data of Pure Substances* (Weinheim: VCH).
Barker, E. S. 1979. Detection of SO_2 in the UV spectrum of Venus. *Geophys. Res. Lett.* 6:117–120.
Barker, E. S., et al. 1975. Relative spectrophotometry of Venus from 3067 to 5960 Å. *J. Atmos. Sci.* 32:1205.
Bauer, S. H., Jeffers, P., Lifshitz, A., and Yavada, B. 1971. Reaction between CO and SO_2 at elevated temperatures: A shock-tube investigation. In *Proc. 13th Symp. on Internal Combustion*, pp. 417–425.
Baulch, D. L., Drysdale, D. D., Duxbury, J., and Grant, S. 1976. *Evaluated Kinetic Data for High Temperature Reactions* (London: Butterworths).
Bertaux, J. L., et al. 1987. Investigation of UV absorption in the atmosphere of Venus at VEGA 1,2 descent probes. *Cosmic Res.* 25(5):691–706.
Bertaux, J. L., et al. 1996. VEGA-1 and VEGA-2 entry probes: An investigation of local UV absorption (220–400 nm) in the atmosphere of Venus (SO_2, aerosols, cloud structure). *J. Geophys. Res.* 101:12709–12745.
Bézard, B., et al. 1993. The abundance of sulfur dioxide below the clouds of Venus. *Geophys. Res. Lett.* 20:1587–1590.
Carlson, R. W., et al. 1991. Galileo infrared imaging spectroscopy measurements at Venus. *Science* 253:1541–1548.
Cimino, J. 1982. The composition and vertical structure of the lower cloud deck on Venus. *Icarus* 51:334–357.
Clancy, R. T., and Muhleman, D. O. 1991. Long-term (1979–1990) changes in the thermal, dynamical, and compositional structure of the Venus mesosphere as inferred from microwave spectral observations of ^{12}CO, ^{13}CO and $C^{18}O$. *Icarus* 89:129–146.
Connes, P., Noxon, J. F., Traub, W. A., and Carleton, N. P. 1979 $O_2(^1\Delta)$ emission in the day and night airglow of Venus. *Astrophys. J. Lett.* 233:29–32.
Conway, R. R., McCoy, R. P., Barth, C. A., and Lane, A. L. 1979. IUE detection of sulfur dioxide in the atmosphere of Venus. *Geophys. Res. Lett.* 6:629–631.
DeMore, W. B., Leu, M. T., Smith, R. H., and Yung, Y. L. 1985 Laboratory studies on the reactions between chlorine, sulfur dioxide, and oxygen: Implications for the Venus stratosphere. *Icarus* 63:347–353.
Deriugin, V. A., et al. 1987. Automatic stations VEGA-1 and VEGA-2. Functioning of descent probes in the atmospheres of Venus. *Cosmic Res.* 25(5):494.
Ekonomov, A. P., et al. 1983. UV photometry at the Venera 13 and 14 landing probes. *Cosmic Res.* 21:194–206.
Esposito, L. W. 1980. Ultraviolet contrasts and the absorbers near the Venus cloud tops. *J. Geophys. Res.* 85:8151–8157.
Esposito, L. W. 1984. Sulfur dioxide shows evidence for Venus volcanism. *Science* 223:1072.
Esposito, L. W., and Travis, L. D. 1982. Polarization studies of the Venus UV contrasts. *Icarus* 51:374–390.
Esposito, L. W., Winick, J. R., and Stewart, A. I. 1979. Sulfur dioxide in the Venus atmosphere: Distribution and implications. *Geophys. Res. Lett.* 6:601–604.
Esposito, L. W., et al. 1983. The clouds and hazes on Venus. In *Venus*, eds. D. M. Hunten, L. Colin, T. M. Donahue and V. I. Moroz (Tucson: Univ. of Arizona Press), 484–564.
Esposito, L. W., et al. 1988. Sulfur dioxide at the Venus cloud tops 1978–1986. *J. Geophys. Res.* 93:5267–5276.
Fegley, B., Jr., and Treiman, A. H. 1992. Chemistry of atmosphere-surface interactions on Venus and Mars. In *Venus and Mars: Atmospheres, Ionsopheres, and Solar Wind Interactions*, AGU Geophysical Mono. 66, pp. 7–71.
Fink, U., Larson, H. P., Kuiper, G. P., and Poppen, R. F. 1972. Water vapor in the atmosphere of Venus. *Icarus* 17:617–631.
Florensky, C. P., Volkov, V., and Nikolaeva, O. 1978. A geochemical model of the Venus troposphere. *Icarus* 33:537–553.
Gel'man, B. G., et al. 1979. Gas chromatograph analysis of the chemical composition of the Venus atmosphere. *Space Res.* 20:219.
Gnedykh, V. I., et al. 1987*a*. Vertical structure of the Venus cloud layer at the VEGA-1 and VEGA-2 landing points. *Kosmich. Issled.* 25:707–714.
Gnedykh, V. I., et al. 1987*b*. Vertical structure of cloud layer above landing sites of VEGA 1 and VEGA 2. *Kosmich. Issled.* 25:707–714 (in Russian).
Giauque, W. F., Horning, E. W., Kunzler, J. E., and Rubin, T. R. 1960. The thermodynamic properties of aqueous sulfuric acid solutions and hydrates from 15 to 300 K. *J. Amer. Chem. Soc.* 82:62–67.
Golovin, Yu. M., Moshkin, B. E., and Ekonomov, A. P. 1981. Aerosol component properties as measured by the Venera 11 and 12 spectrophotometer. *Cosmic Res.* 19:295–302.
Hapke, B., and Graham, F. 1985. Disulfur Monoxide and the spectra of Io and Venus. *Lunar Planet. Sci.* XV:316–317 (abstract).
Hapke, B., and Graham, F. 1989. Spectral properties of condensed phases of disulfur monoxide, polysulfur oxide, and irradiated sulfur. *Icarus* 79:47–55.
Hapke, B. W., and Nelson, R. M. 1975. Evidence for an elemental sulfur component of the clouds from Venus spectroscopy. *J. Atmos. Sci.* 32:1212–1218.
Hartley, K. K., Wolf, A. R., and Travis, L. D. 1989. Croconic acid: An absorber in the Venus clouds? *Icarus* 77:382–390.
Hoffman, J. H., Hodges, R. R., Jr., Donahue, T. M., and McElroy, M. B. 1980. Composition of the Venus lower atmosphere from the Pioneer Venus mass spectrometer. *J. Geophys. Res.* 85:7882–7890.
Hunten, D. M., Colin, L., Donahue, T. M., and Moroz, V. I., eds. 1983. *Venus* (Tucson: Univ. of Arizona Press).
Jenkins, J. M. 1992. Variations in the 13-cm Opacity Below the Main Cloud Layer in the Atmosphere of Venus Inferred from the Pioneer-Venus Radio Occultation Studies 1978–1992. Ph.D. Thesis, Georgia Inst. of Technology.
Jenkins, J. M., et al. 1994. Radio occultation studies of the Venus atmosphere with the Magellan spacecraft. *Icarus* 110:79–94.
Kamp, L. W., and Taylor, F. W. 1990. Radiative-transfer models of the night side of Venus. *Icarus* 86:510–529.
Knollenberg, R. G., and Hunten, D. M. 1980. Results of the Pioneer Venus particles size spectrometer experiment. *J. Geophys. Res.* 85:8039–8058.
Knollenberg, R. G., et al. 1980. The clouds of Venus: A synthesis report. *J. Geophys. Res.* 85:8059–8081.
Kondratiev, V. N. 1971. *Rate Coefficients of Gas Phase Reactions* (Moscow: Nauka Press).
Krasnopolsky, V. A. 1985. Chemical composition of Venus' clouds. *Planet. Space Sci.* 33:109–117.
Krasnopolsky, V. A. 1986. *Photochemistry of the Atmospheres of Mars and Venus* (New York: Springer-Verlag).
Krasnopolsky, V. A. 1989. Vega mission results and chemical composition of Venusian clouds. *Icarus* 80:202–210.
Krasnopolsky, V. A., and Parshev, V. A. 1979. On the chemical composition of the troposphere and cloud layer of Venus based on the Venera 11 and 12 and Pioneer Venus measurements. *Cosmic Res.* 17:763–770.
Krasnopolsky, V. A., and Parshev, V. A. 1981*a*. Initial data of calculation of chemical

composition of the Venus atmosphere down to 50 km. *Cosmic Res.* 19:87–109.
Krasnopolsky, V. A., and Parshev, V. A. 1981*b*. Photochemistry of the Venus atmosphere down to 50 km: Results of calculations. *Cosmic Res.* 19(2):61–280.
Krasnopolsky, V. A., and Parshev, V. A. 1983. Photochemistry of the Venus atmosphere. In *Venus*, eds. D. M. Hunten, L. Colin, T. M. Donahue and V. I. Moroz (Tucson: Univ. Arizona Press), pp. 431–458.
Krasnopolsky, V. A., and Pollack, J. B. 1994. H_2O-H_2SO_4 system in Venus' clouds and OCS, CO, and H_2SO_4 profiles in Venus' troposphere. *Icarus* 109:58–78.
Kumar, S., and Taylor, H. A. 1985. Deuterium on Venus: Model comparisons with Pioneer Venus observations of the predawn bulge ionosphere. *Icarus* 62:494–504.
Kumar, S., Hunten, D. M., and Taylor, H. A. 1981. H_2 abundance in the atmosphere of Venus. *Geophys. Res. Lett.* 8:237–239.
Kunde, V. G., Hanel, R. A., and Herath, L. W. 1977. High spectral resolution ground-based observations of Venus in the 450–1250 cm^{-1} region. *Icarus* 32:210–224.
Levine, J. S., et al. 1982. Production of nitric oxide by lightning on Venus. *Geophys. Res. Lett.* 9:893–896.
Lewis, J. S. 1970. Venus: atmospheric and lithospheric composition. *Earth Planet. Sci. Lett.* 10:73–80.
Linkin, V. M., et al. 1985. VENERA 15 and VENERA 16 infrared experiment. 5. Preliminary results of analysis of brightness temperature and thermal flux fields. *Cosmic Res.* 23(2):212–221.
Marov, M. Ya., et al. 1983. Study of Venus cloud structure by the Venera 13 and 14 nephelometers. *Cosmic Res.* 21:207–215.
McClintock, W. E., Barth, C. A., and Kohnert, R. A. 1994. Sulfur dioxide in the atmosphere of Venus: Sounding rocket observations. *Icarus* 112:381–388.
McElroy, M., Prather, M., and Rodriguez, J. 1982. Escape of hydrogen from Venus. *Science* 215:1614–1615.
Moroz, V. I. 1987. Scientific results of the VEGA mission. *Kosmich. Issled.* 25:659–672 (in Russian).
Moroz, V. I., et al. 1983. The Venera 13 and 14 spectrophotometric experiment. II. Preliminary analysis of H_2O absorption bands in spectra. *Cosmic Res.* 21:187–194.
Moroz, V. I., et al. 1985. VENERA 15 and VENERA 16 infrared experiment. 4. Preliminary results of spectral analyses in the region of H_2O and SO_2 absorption bands. *Cosmic Res.* 23(2):202–211.
Moroz, V. I., D. et al. 1986. Venus spacecraft infrared radiance spectra. Some aspects of their interpretation. *Applied Opt.* 25(10).
Moroz, V. I., et al. 1990. Water vapor and sulfur dioxide abundances at the Venus cloud tops from the VENERA 15 infrared spectrometry data. *Adv. Space Res.* 10(5):77.
Moshkin, B. E., et al. 1983. Veneras 13 and 14 spectrophotometric experiment. I. Methodics, results, and preliminary analysis of the measurements. *Cosmic Res.* 21:177–186.
Na, C. Y. 1992. Sulfur Oxides in the Middle Atmosphere of Venus. Ph.D Thesis, Univ. of Colorado.
Na, C. Y., and Esposito, L. W. 1996. UV observations of Venus with HST. In preparation.
Na, C. Y., Esposito, L. W., and Skinner, T. E. 1990. International Ultraviolet Explorer observation of Venus SO_2 and SO. *J. Geophys. Res.* 95:7485.
Na, C. Y., Esposito, L. W., McClintock, W. E., and Barth, C. A. 1994. Sulfur dioxide in the atmosphere of Venus: Modeling results. *Icarus* 112:389–395.
Oertel, D., et al. 1985. VENERA-15 and VENERA-16 infrared experiment. 1. Technique and first results. *Cosmic Res.* 23(2):162–175.

Oertel, D., et al. 1987. Infrared spectrometry from VENERA-15 and VENERA-16. *Adv. Space Res.* 5(9):25.
Owen, T., and Sagan, C. 1972. Minor constituents in planetary atmospheres: Ultraviolet spectroscopy from the Orbiting Astronomical Observatory. *Icarus* 16:557–568.
Oyama, V. I., et al. 1980. Pioneer Venus gas chromatography at the lower atmosphere of Venus. *J. Geophys. Res.* 85:7891–7902.
Petryanov, I. V., et al. 1981. Iron in the Venus clouds. *Dokl. AN SSSR* 260:834.
Pollack, J. B., et al. 1978. Properties of the clouds of Venus as inferred from airborne observations of its near infrared reflectivity spectrum. *Icarus* 34:28–45.
Pollack, J. B., et al. 1980. Distribution and source of the UV absorption in Venus atmosphere. *J. Geophys. Res.* 85:8141–8150.
Pollack, J. B., et al. 1993. Near-infrared light from Venus' nightside: A spectroscopic analysis. *Icarus* 103:1–42.
Porshnev, N. V., et al. 1987. Gas chromatographic analysis of products of thermal reactions of the cloud aerosol of Venus by the Vega 1 and 2 probes. *Cosmic Res.* 25:715.
Prinn, R. G. 1975. Venus: chemical and dynamical processes in the stratosphere and mesosphere. *J. Atmos. Sci.* 32:1237–1247.
Prinn, R. G. 1978. Venus: chemistry of the lower atmosphere prior to the Pioneer Venus mission. *Geophys. Res. Lett.* 5:973–976.
Prinn, R. G. 1979. On the possible role of gaseous sulfur and sulfanes in the atmosphere of Venus. *Geophys. Res. Lett.* 6:807–810.
Prinn, R. G. 1985. The photochemistry of the atmosphere of Venus. In *The Photochemistry of Atmospheres*, ed. J. S. Levine (Orlando: Academic Press), pp. 281–336.
Ragent, B., and Blamont, J. E. 1980. The structure of the clouds of Venus: Results of the Pioneer Venus nephelometric experiment. *J. Geophys. Res.* 85:8089–8105.
Reed, R. A., Forrest, W. J., Houck, J. R., and Pollack, J. B. 1978. Venus: The 17 to 38 micron spectrum. *Icarus* 33:554–557.
Rodriguez, J. M., Prather, M. J., and McElroy, M. B. 1984. Hydrogen on Venus: Exospheric distribution and escape. *Planet. Space Sci.* 32:1235–1251.
Rossow, W. B., et al. 1980. Cloud Morphology and Motions from Pioneer Venus images. *J. Geophys. Res.* 85:8107–8128.
Sagdeev, R. Z., et al. 1986. Overview of VEGA Venus balloon in situ meteorological measurements. *Science* 231:1411–1413.
Schaefer, K., et al. 1987. Structure of the middle atmosphere of Venus from analyses of Fourier-spectrometer measurements aboard VENERA-15. *Adv. Space Res.* 7(12):17.
Schaefer, K., et al. 1990. Infrared Fourier Spectrometer experiment from VENERA-15. *Adv. Space Res.* 10(5):57.
Schofield, J. T., Taylor, F. W., and McCleese, D. J. 1982. The global distribution of water vapor in the middle atmosphere of Venus. *Icarus* 52:263–278.
Sill, G. T. 1983. The clouds of Venus: sulfuric acid by the lead chamber process. *Icarus* 53:10.
Spankuch, D., et al. 1985. VENERA-15 and VENERA-16 infrared experiment. 2. Preliminary results of temperature profile retrieval. *Cosmic Res.* 23(2):176–188.
Spankuch, D., Matsygorin, I. A., Dubois, R., and Zasova, L. V. 1990. Venus middle-atmosphere temperature from VENERA-15. *Adv. Space Res.* 10(5):67.
Stewart, A. I. F., Anderson, D. E., Esposito, L. W., and Barth, C. A. 1979. Ultraviolet spectroscopy of Venus: Initial results from the Pioneer Venus Orbiter. *Science* 203:777–778.
Surkov, Yu. A., et al. 1981. A study of the Venus cloud aerosol by Venera 12

(preliminary data). *Cosmic Res.* 20:435.
Surkov, Yu. A., Ivanova, V. F., Pudov, A. N., and Caramel, D. 1987. Determination of the aerosols chemical composition in the Venusian clouds by means of the mass-spectrometer MALAHIT on the VEGA-1 probe. *Kosmich. Issled.* 15:744–750 (in Russian).
Sze, N. D., and McElroy, M. B. 1975. Some problems in Venus' aeronomy. *Planet. Space Sci.* 23:763–786.
Taylor, F. W., et al. 1980. Structure from the Pioneer Venus Orbiter. *J. Geophys. Res.* 85:7963–8006.
Titov, D. V. 1983. On the possibility of aerosol formation by the reaction between SO_2 and NH_3 in Venus' atmosphere. *Cosmic Res.* 21:401.
Tomasko, M. G., Doose, L. R., Smith, P. H., and Odell, A. P. 1980. Measurements of the flux of sunlight in the atmosphere of Venus. *J. Geophys. Res.* 85:8167–8186.
Toon, O. B., Turco, R. P., and Pollack, J. B. 1982. The ultraviolet absorber on Venus: Amorphous sulfur. *Icarus* 51:358.
Traub, W. A., and Carleton, N. P. 1974. A search for H_2O and O_2 on Venus. In *Exploration of Planetary Atmospheres*, eds. A. Woszcyk and C. Iwanishewska (Dordrecht: D. Reidel), p. 223.
Trauger, J. T., and Lunine, J. I. 1983. Spectroscopy of molecular oxygen in the atmospheres of Venus and Mars. *Icarus* 55:272.
Volkov, V. P., Sidorov, Y. I., Khodakovsky, I. L., and Barsukov, V. L. 1982. On the possible condensates in the Venus main cloud layer. *Geokhimia* 3.
von Zahn, U., Kumar, S., Niemann, H., and Prinn, R. G. 1983. Composition of the Venus atmosphere. In *Venus*, eds. D. M. Hunten, L. Colin, T. M. Donahue and V. I. Moroz (Tucson: Univ. of Arizona Press), pp. 299–430.
Watson, A. J., et al. 1979. Oxides of nitrogen and the clouds of Venus. *Geophys. Res. Lett.* 6:743–746.
Widemann, T., Bertaux, J. L., Moroz, V. I., and Ekonomov, A. P. 1993. VEGA-1 and VEGA-2 descent modules: In-situ measurements of ultraviolet absorption and relationship with present active volcanism on Venus. *Bull. Amer. Astron. Soc.* 25:1094 (abstract).
Winick, J. R., and Stewart, A. I. 1980. Photochemistry of SO_2 in Venus' upper cloud layers. *J. Geophys. Res.* 85:7849–7860.
Young, A. T. 1977. An improved Venus cloud model. *Icarus* 32:1–26.
Young, A. T. 1983. Venus cloud microphysics. *Icarus* 56:568.
Yung, Y. L., and DeMore, W. B. 1982. Photochemistry of the stratosphere of Venus: Implications for atmospheric evolution. *Icarus* 51:199–247.
Zasova, L. V., Krasnopolsky, V. A., and Moroz, V. I. 1981. Vertical distribution of SO_2 in the upper cloud layer of Venus and origin of the UV absorption. *Adv. Space Res.* 113–16.
Zasova, L. V., et al. 1985. VENERA-15 and VENERA-16 infrared experiment. 3. Some spectral analyses results on the cloud structure. *Cosmic Res.* 23(2):189.
Zasova, L. V., et al. 1989. Venusian clouds from VENERA-15 data. *Veroffenlichungen Forschungsbereichs Geo- Kosmoswissenschaften*, 18 (Berlin: Academie-Verlag).
Zasova, L. V., Moroz, V. I., Esposito, L. W., and Na, C. Y. 1993. SO_2 in the middle atmosphere of Venus: IR measurements from VENERA-15 and comparison to UV data. *Icarus* 105:92–109.
Zhulanov, Yu. V., Mukhin, L. M., and Nenarokov, D. F. 1986. Preliminary results of particles number densities measurements on clouds of Venus on heights 47–63 km on board VEGA-1 and VEGA-2 landing probes. *Pisma Astron. Z.* 12:97–130.

THE GENERAL CIRCULATION OF THE VENUS ATMOSPHERE: AN ASSESSMENT

P. J. GIERASCH
Cornell University

R. M. GOODY
Harvard University

R. E. YOUNG
NASA Ames Research Center

D. CRISP, C. EDWARDS, R. KAHN, D. McCLEESE and D. RIDER
Jet Propulsion Laboratory

A. DEL GENIO
Goddard Institute for Space Studies

R. GREELEY
Arizona State University

A. HOU
NASA Goddard Space Flight Center

C. B. LEOVY
University of Washington

and

M. NEWMAN
University of Colorado

The overall spin or "superrotation" of the Venus atmosphere is a striking phenomenon. In the 15 years since the NASA Pioneer Venus mission, a first-order understanding has been reached of the dynamics of the atmospheric region near and just above the Venus cloud tops. Tidal motions induced by solar heating produce a traveling disturbance whose vertical momentum transports are balanced by mean flow advection. The balance explains the shear of the mean flow above the clouds, and partially explains the strength of the mean flow at the cloud level where the strongest superrotation of